

Mohammad Yuzariyadi  
& Kosuke Heki  
Hokkaido University,  
Sapporo, Japan

EGU-2020

# Enhancement of Interplate Coupling in Adjacent Segments after Recent Megathrust Earthquakes

**Abstract.** The concept of a stressed elastic lithospheric plate riding on a viscous asthenosphere is used to calculate the recurrence interval of great earthquakes at convergent plate boundaries, the separation of decoupling and lithospheric earthquakes, and the migration pattern of large earthquakes along an arc. It is proposed that plate motions accelerate after great decoupling earthquakes and that most of the observed plate motions occur during short periods of time, separated by periods of relative quiescence.

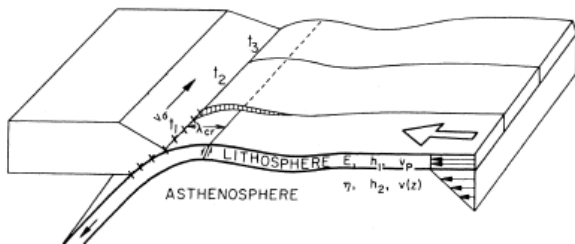
From the magnetic record sea floor spreading appears to be uniform over periods of many millions of years. However, from seismic data we know that motions at plate boundaries are not continuous, but occur mainly in jerks separated by tens to hundreds of years. It also appears that major earthquakes are not random in time and location but have some relation to each other. Mogi (1), in particular, has investigated the time-space sequence of global seismic activity and has proposed several migration patterns. For example, active seismic areas migrated systematically from Japan to Alaska in the last 35 years, during which this seismic belt was almost completely covered by aftershock areas of great earthquakes. Another pattern started in Central America and migrated to southern Chile in the same period of time. Migration velocities in these belts are 150 to 270 km/year. A particularly clear example of earthquake migration occurred on the Anatolian fault in Turkey after the great earthquake of 1939. The average migration rate, 50 to 100 km/year, has decreased with time. It has been suggested (2) that variations in the rotation rate of the earth and great decoupling earthquakes may be related to the start of a migration pattern.

In this report I quantify some of the implications of a simple model of an elastic plate riding on a viscous foundation. This model can be used to estimate the recurrence interval of large earthquakes, the time interval between large earthquakes along an arc, and the distance between decoupling and lithospheric (3) earthquakes. The model shows that relative plate rates can be calculated from seismicity only if long enough periods of time are considered.

diffusion. Recurrence rates can be estimated from a simple elastic model involving the loading of a plate.

Kanamori (3) introduced the concepts of decoupling and lithospheric earthquakes. The first are trench earthquakes in which the boundary between the underthrusting plate and the adjacent restraining plate is broken, temporarily decoupling the two converging lithospheres. A lithospheric earthquake is one that breaks the entire oceanic lithosphere, seaward of the trench. What are the consequences of a great decoupling earthquake? First, one would expect accelerated plate motions in the vicinity of the trench. In fact, are observed earthquakes stands of the earthquake per year has large earthquakes underthrusting of the down approach can be expected. Frictional contact between the oceanic and continental lithospheres is reduced. Continental rebound (sinking) and reduction of the oceanic lithospheric bulge (6), previously supported by the

relieved stresses, will also occur. The second consequence is that the stress discontinuity resulting from the earthquake will diffuse away from the fault plane and trigger activity along adjacent parts of the arc. In a purely elastic situation this information will flow at elastic wave speeds, and adjacent segments of the arc will know within seconds or minutes that they must support more of the stress imposed by the approaching lithosphere; the immediate aftershocks are presumably triggered by this mechanism. In an elastic layer over a viscous asthenosphere part of the information travels more slowly and damps rapidly. Adjacent segments of the arc will be stressed at a more rapid rate than before the decoupling earthquake, because of both accelerated oceanic plate motions in the vicinity of the decoupling earthquake and the stress wave diffusion from the earthquake. The critical distance,  $\lambda_{cr}$ , from the boundary between the plates (the location of the decoupling earthquake)



## Postseismic Enhanced Coupling (found by GNSS in Japan and Chile)

### Geophysical Research Letters

**RESEARCH LETTER**  
10.1002/2016GL071845

This article is a companion to Loveless [2017] doi:10.1002/2017GL072525.

#### Key Points:

- A decade of GPS measurements across the Andes image the megathrust seismic cycle before and between two

## Accelerated subduction? (hypothesized by Heki and Mitsui, 2013)



Contents lists available at SciVerse ScienceDirect

Earth and Planetary Science Letters

journal homepage: [www.elsevier.com/locate/epsl](http://www.elsevier.com/locate/epsl)



## Accelerated Pacific plate subduction following interplate thrust earthquakes at the Japan trench

Kosuke Heki\*, Yuta Mitsui

ku, Sapporo 060 0810, Japan



## The super-interseismic phase of the megathrust earthquake cycle in Chile

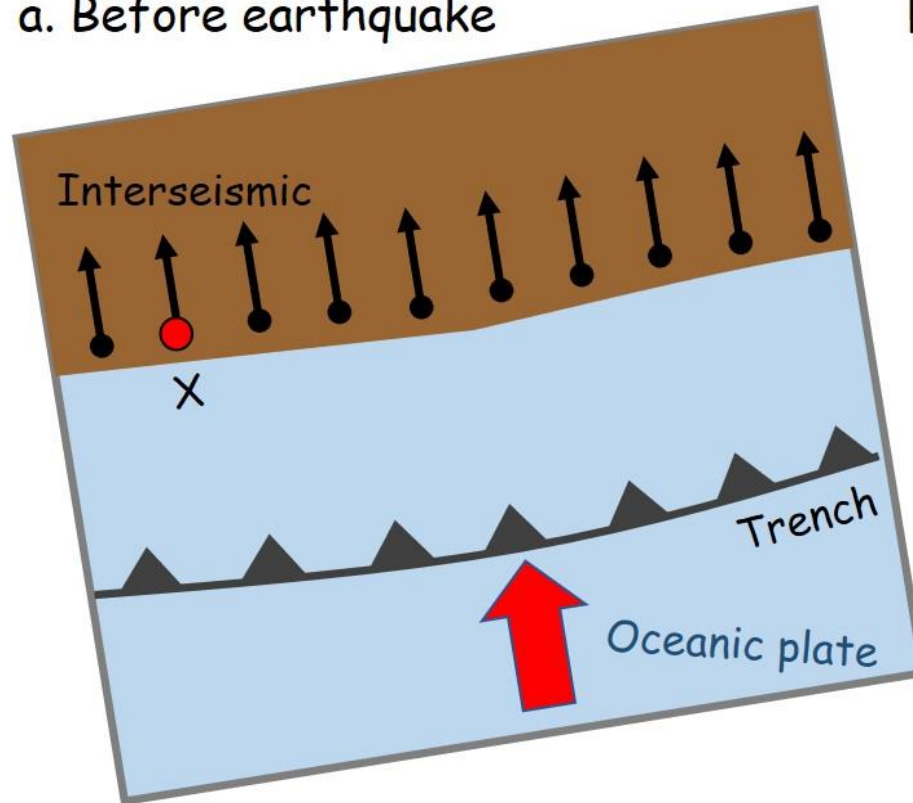
Daniel Melnick<sup>1,2</sup>, Marcos Moreno<sup>3</sup>, Javier Quinteros<sup>3</sup>, Juan Carlos Baez<sup>4</sup>, Zhiguo Deng<sup>3</sup>, Shaoyang Li<sup>3</sup>, and Onno Oncken<sup>3</sup>

<sup>1</sup>Institute of Earth and Environmental Sciences, University of Potsdam, Potsdam, Germany, <sup>2</sup>Instituto de Ciencias de la Tierra, TAQUACH, Universidad Austral de Chile, Valdivia, Chile, <sup>3</sup>GFZ Helmholtz Centre Potsdam, Potsdam, Germany, <sup>4</sup>Centro Sismológico Nacional, Universidad de Chile, Santiago, Chile

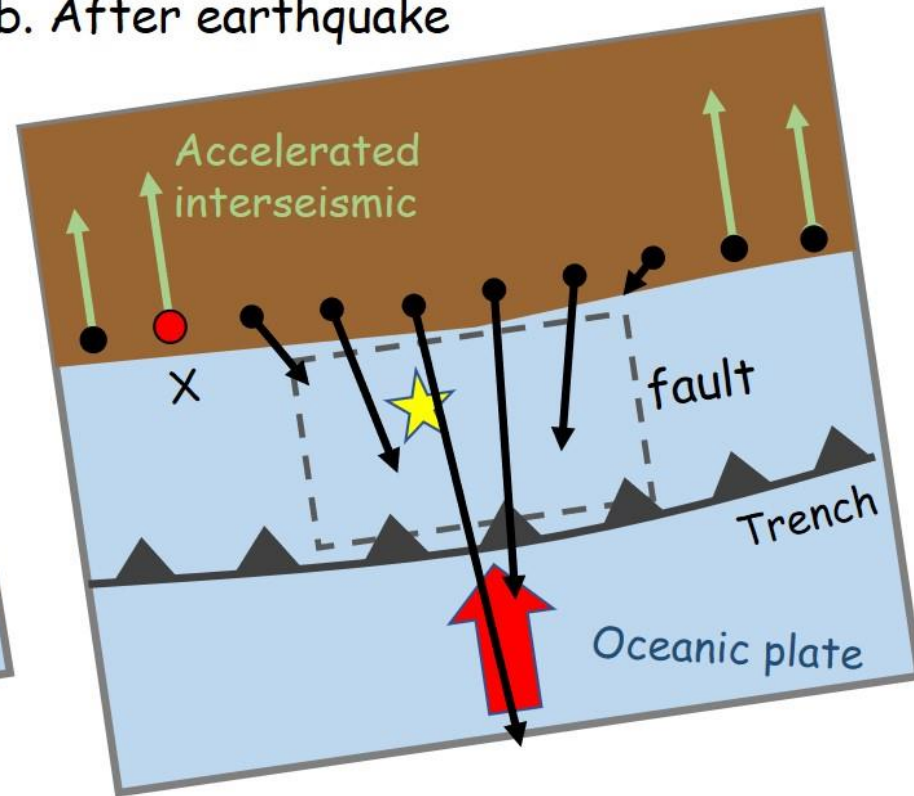
# What kind of phenomenon?

Accelerated landward movement in the neighboring segments of the rupture

a. Before earthquake



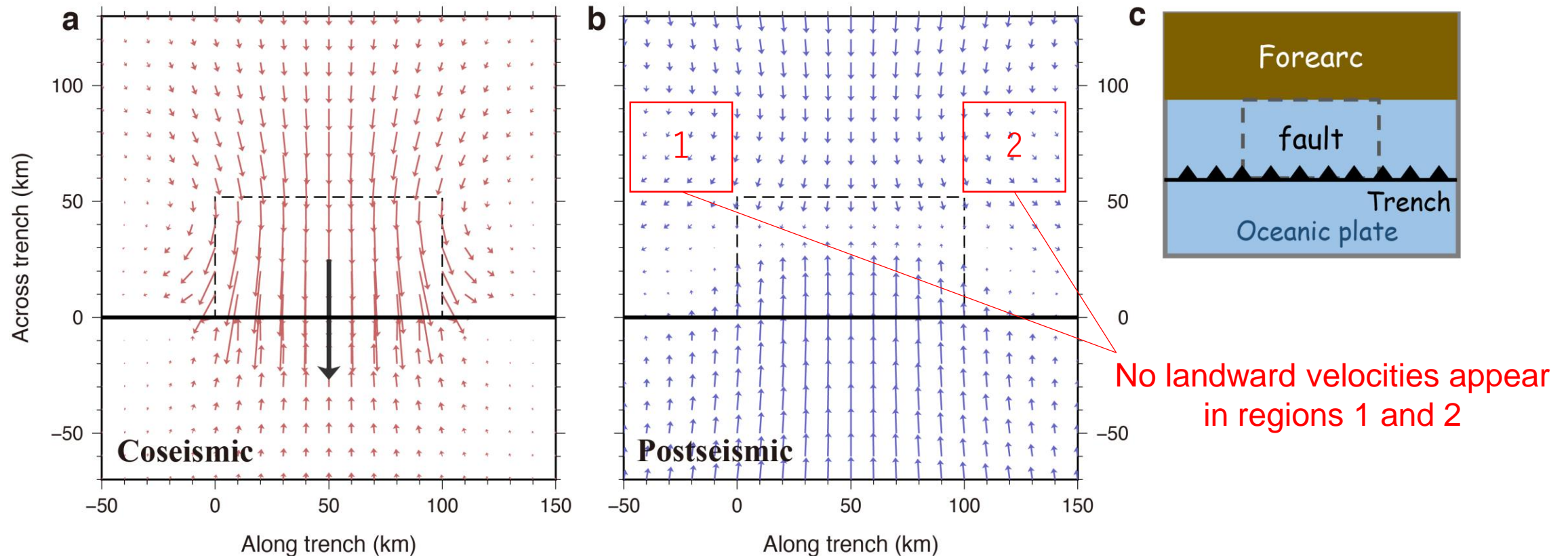
b. After earthquake



This phenomenon cannot be explained by simple viscoelastic relaxation?

# Can viscoelastic relaxation explain it?

Postseismic viscoelastic relaxation generates only trenchward movement for forearc GNSS stations.



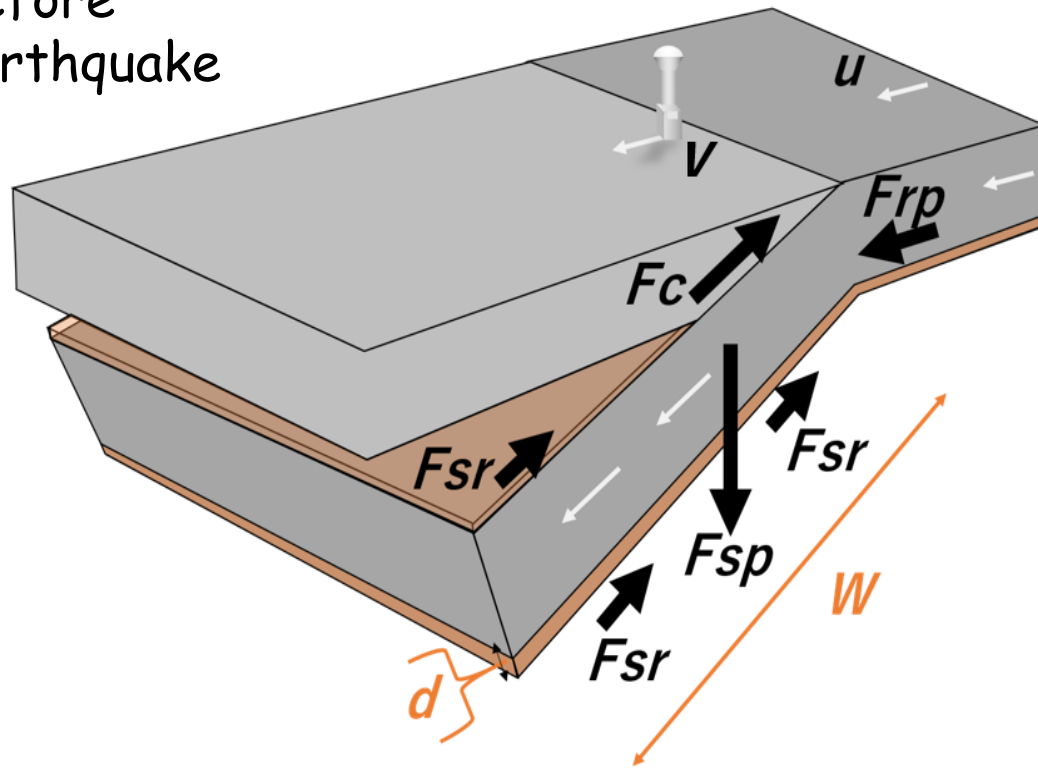
Calculated using the software package by Fukahata and Matsu'ura (2005; 2006)

These landward velocities need to be explained by some other mechanisms.



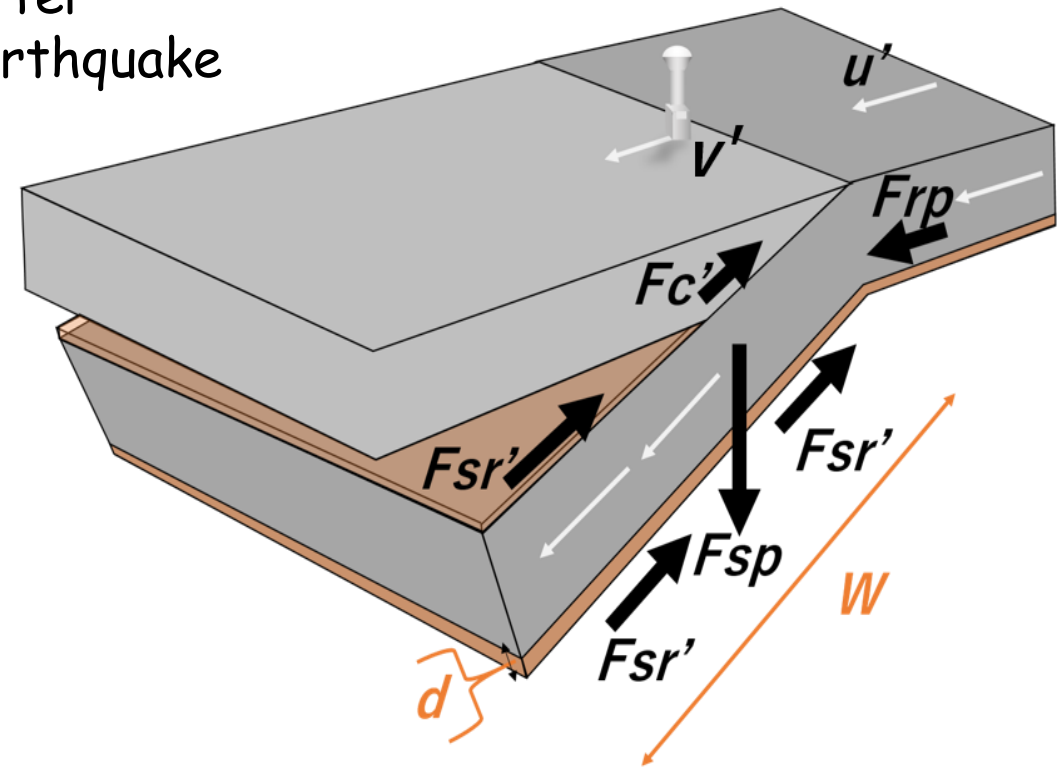
# Slab acceleration model by Heki and Mitsui (2013 EPSL)

Before  
earthquake



Slab pull  $F_{sp}$  balances with plate coupling  $F_c$   
and viscous traction  $F_{sr}$

After  
earthquake



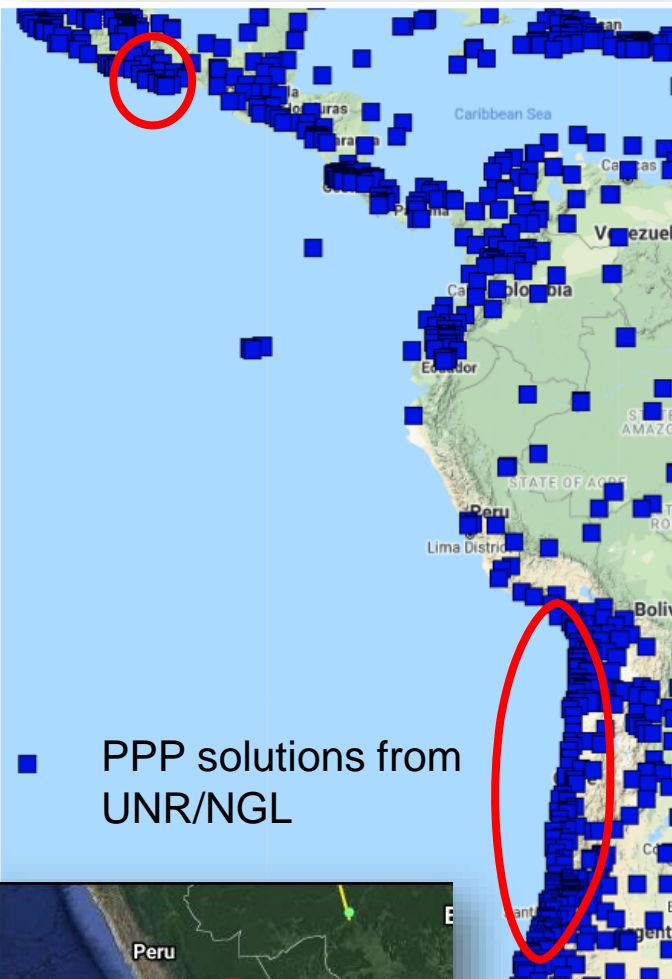
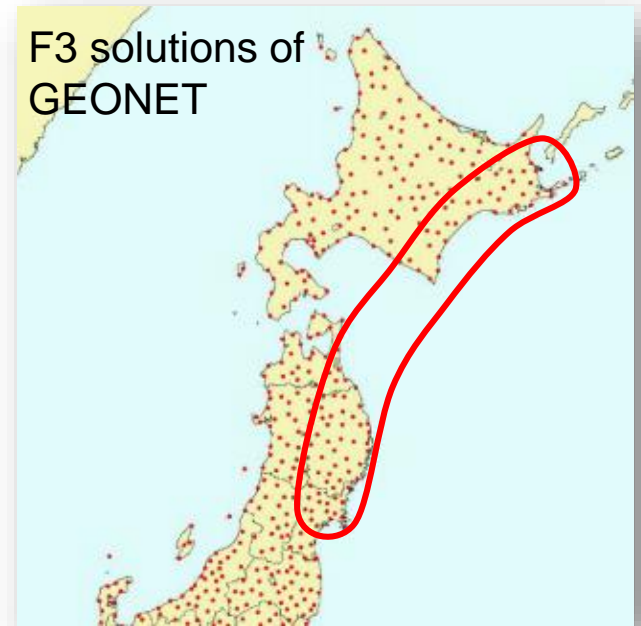
Reduced coupling compensated by increase of viscous traction realized by acceleration

*Fsp*: slab pull, *Frp*: ridge push, *Fc*: interplate coupling, *Fsr*: side resistance, *v*: surface velocity, *u*: slab velocity, *W*: Total trench-normal length of slab where viscous braking works, *d* is the thickness of the thin low viscosity layer at the lithosphere-asthenosphere boundary,  $\mu$ : viscosity of the low-viscosity layer.

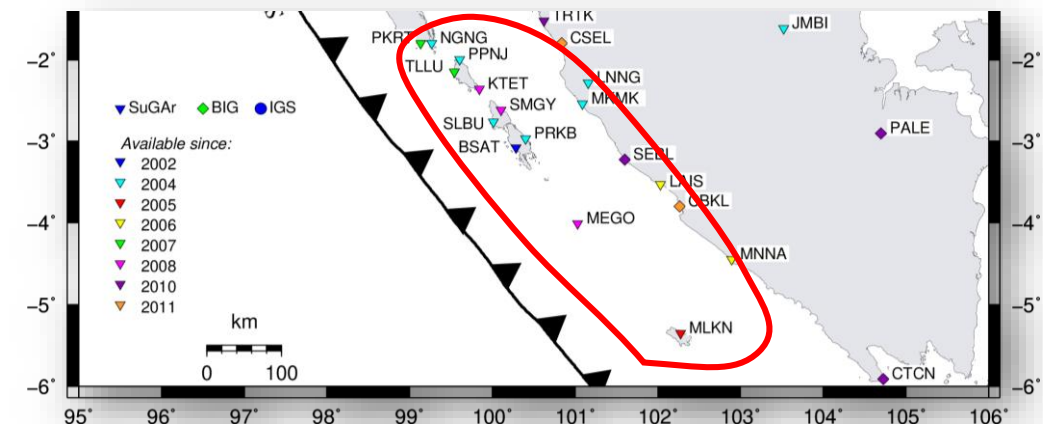
# Data and Method

# GNSS Data

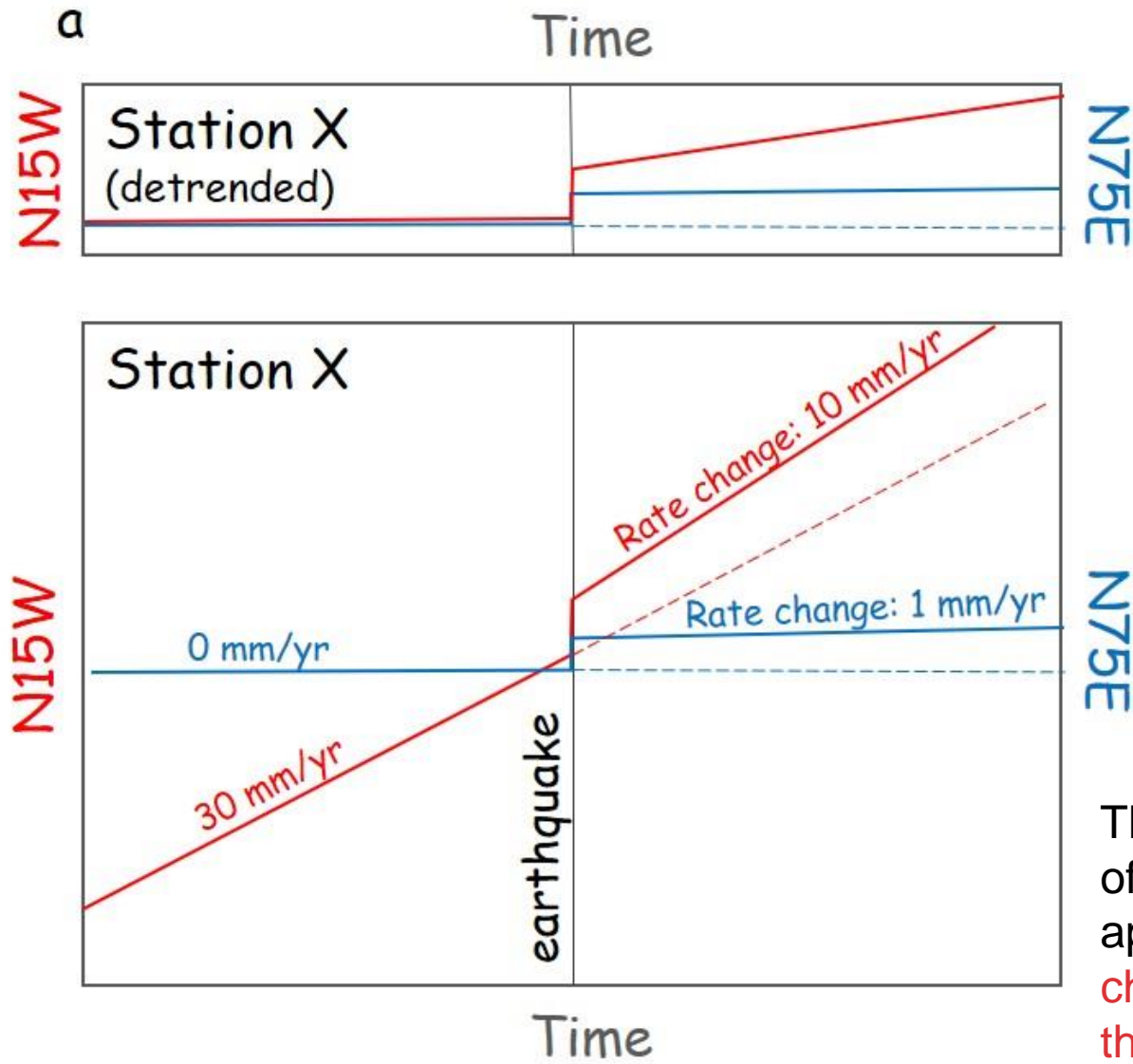
We analyze GNSS daily coordinate data available in forearc regions of subduction zones, western Sumatra, NE Japan, central and northern Chile, and Oaxaca, Mexico.



The Sumatran GPS Array (SuGAR)  
solutions by GAMIT 10.5 by ITB

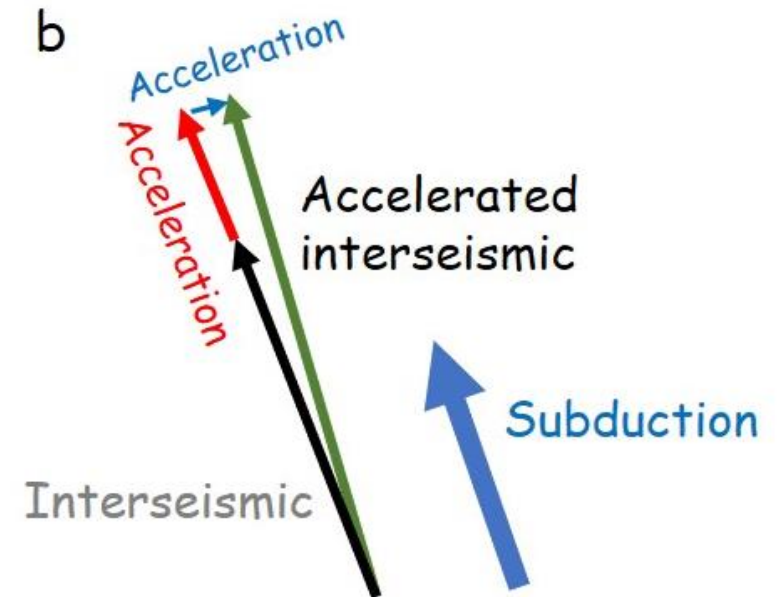


ITRF velocities converted to  
those relative to the landward  
plate using nnr-MORVEL56



# Acceleration diagram

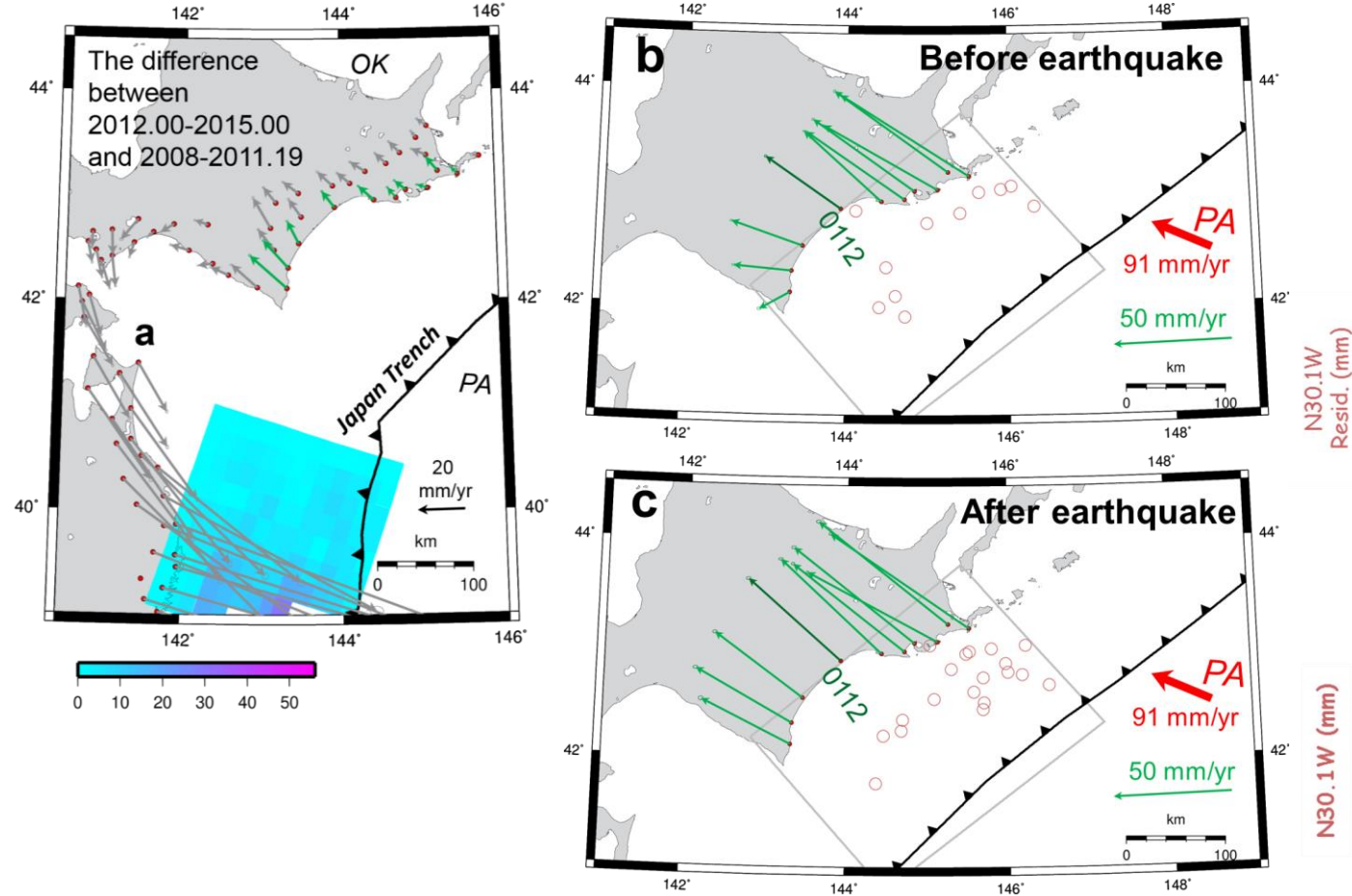
We rotate the two horizontal axes (north and east) so that the two components coincide with the direction **parallel** or **perpendicular** to the interseismic movement of the station before the earthquakes (normally in the direction of the subducting oceanic plate).



The coseismic increase of the landward velocity appears as the **positive change in the slope of the red time series**

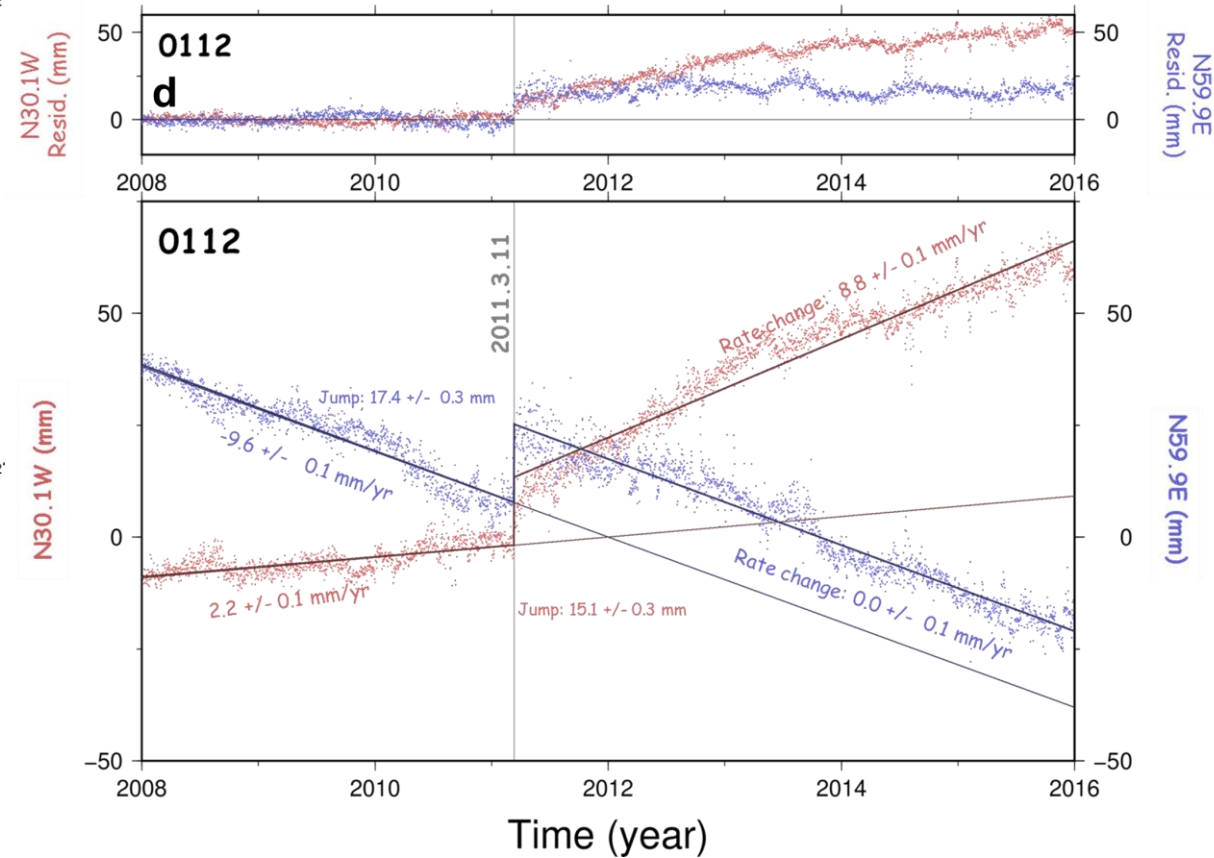


6 cases in 4 subduction zones of postseismic enhancement of interplate coupling



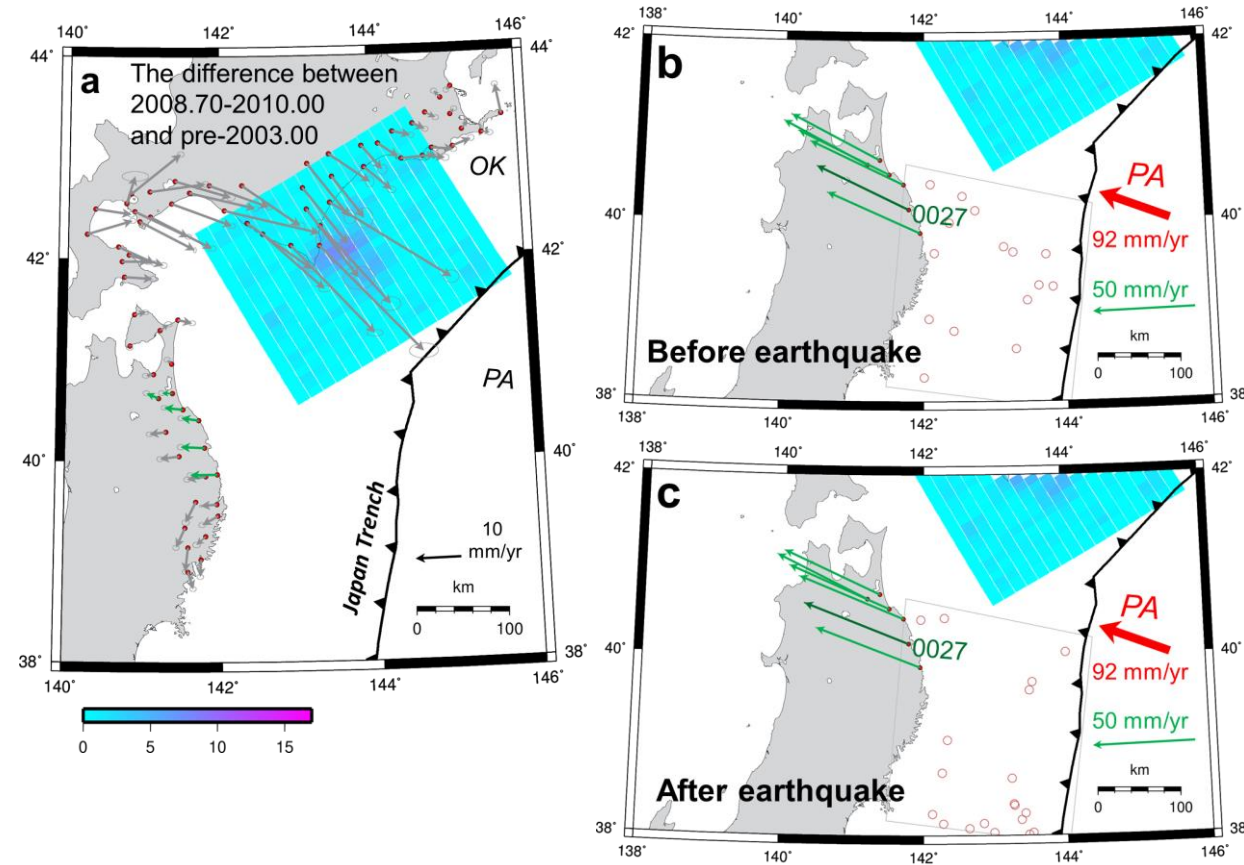
The pre-earthquake landward movement of the GNSS stations has been accelerated after the 2011 Tohoku-oki earthquake.

## The 2011 Tohoku-oki earthquake ( $M_w$ 9.0)

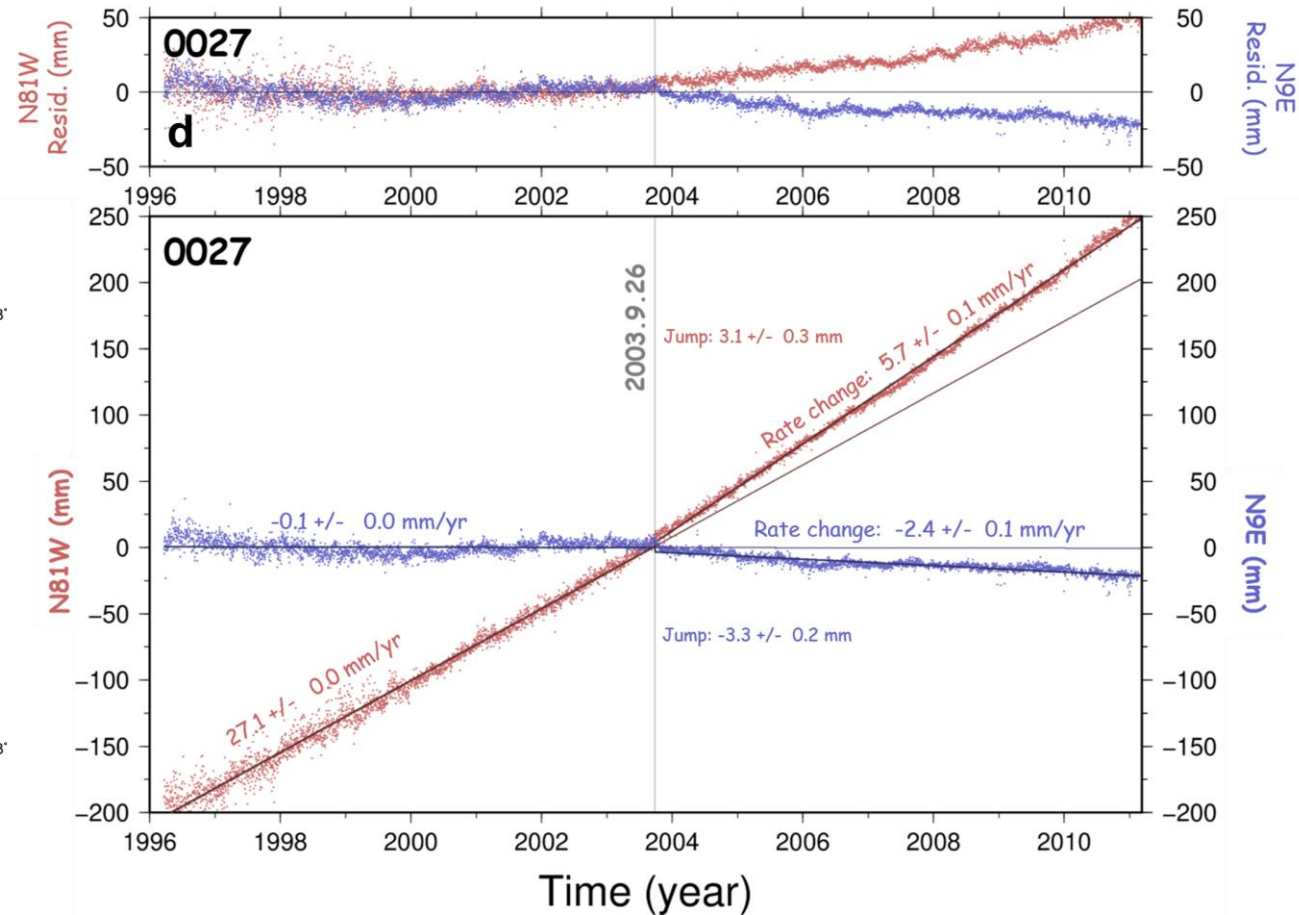


Positive change in the slope of the red time series.

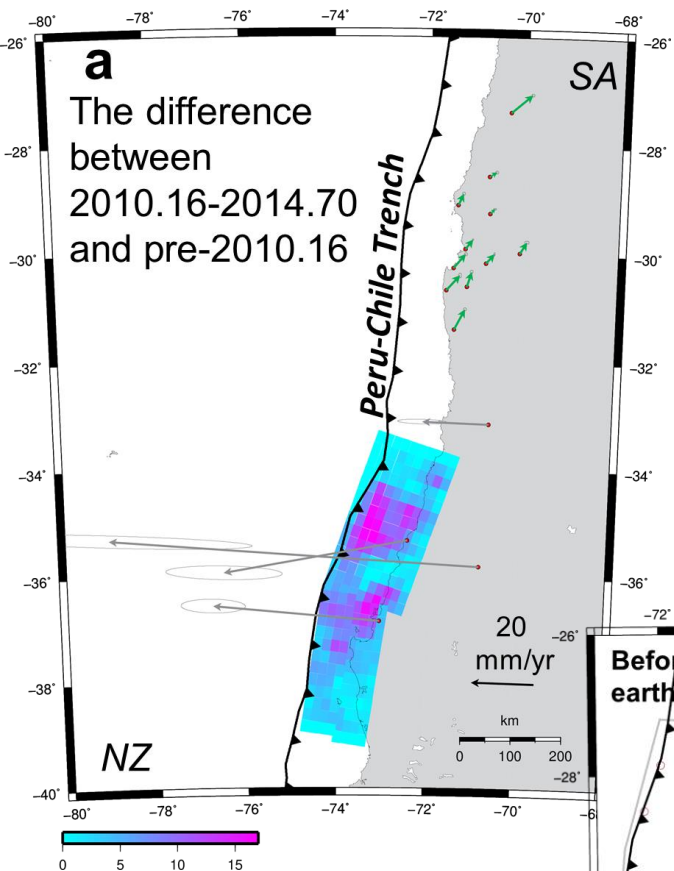
# The 2003 Tokachi-oki Earthquake (Mw 8.3)



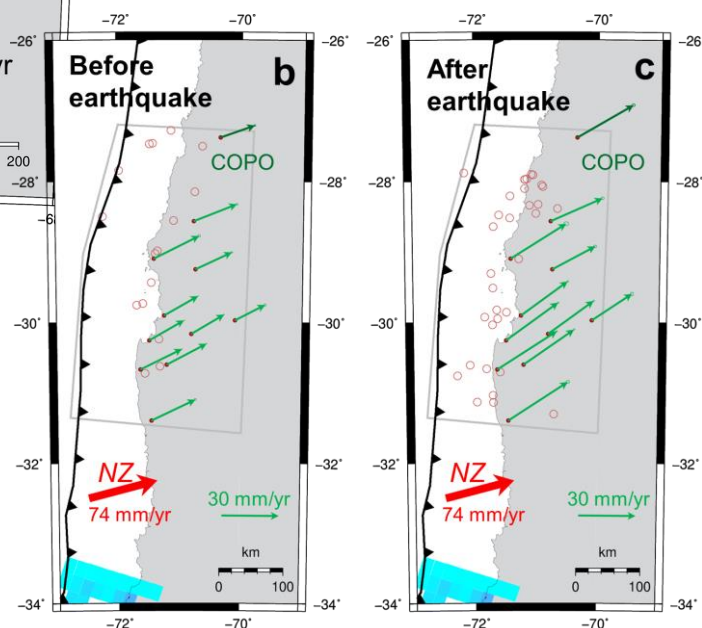
The pre-earthquake landward movement of the GNSS stations has been accelerated after the 2003 Tokachi-oki earthquake.



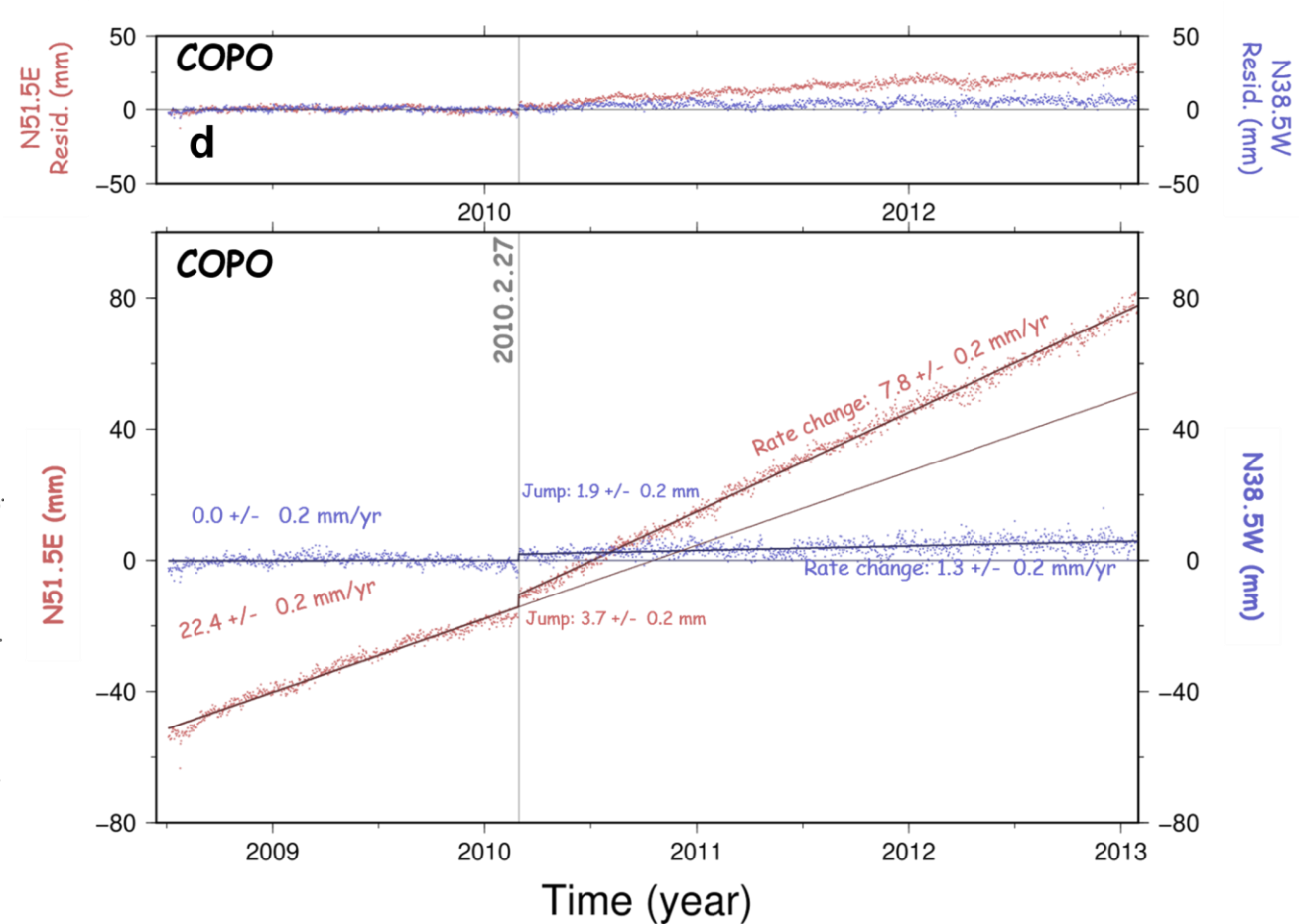
Positive change in the slope of the red time series.



The pre-earthquake landward movement of the GNSS stations has been accelerated after the 2010 Maule earthquake.

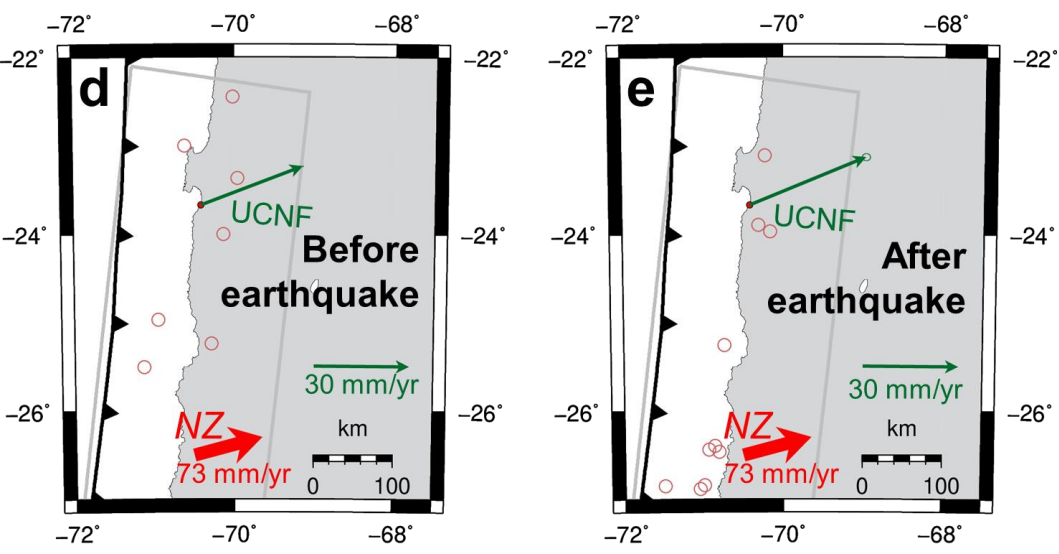
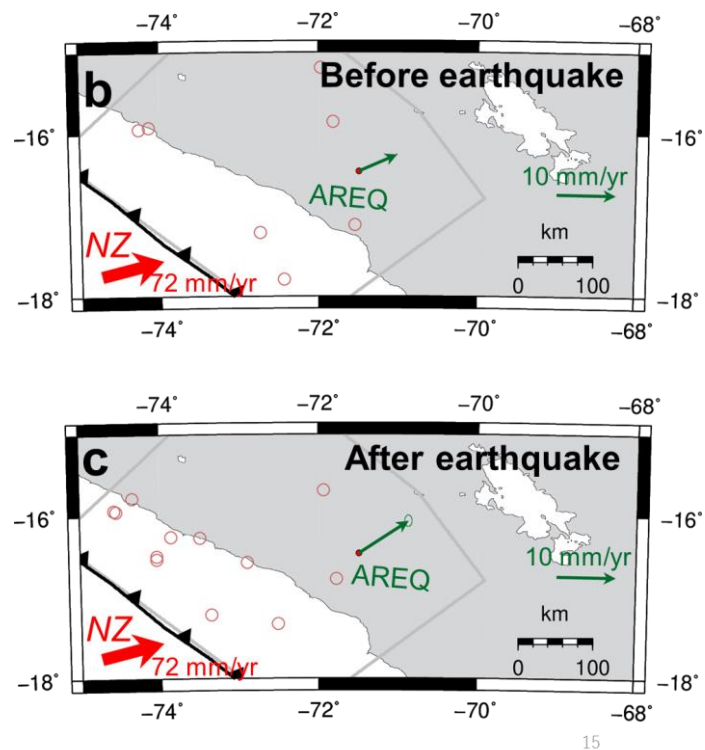
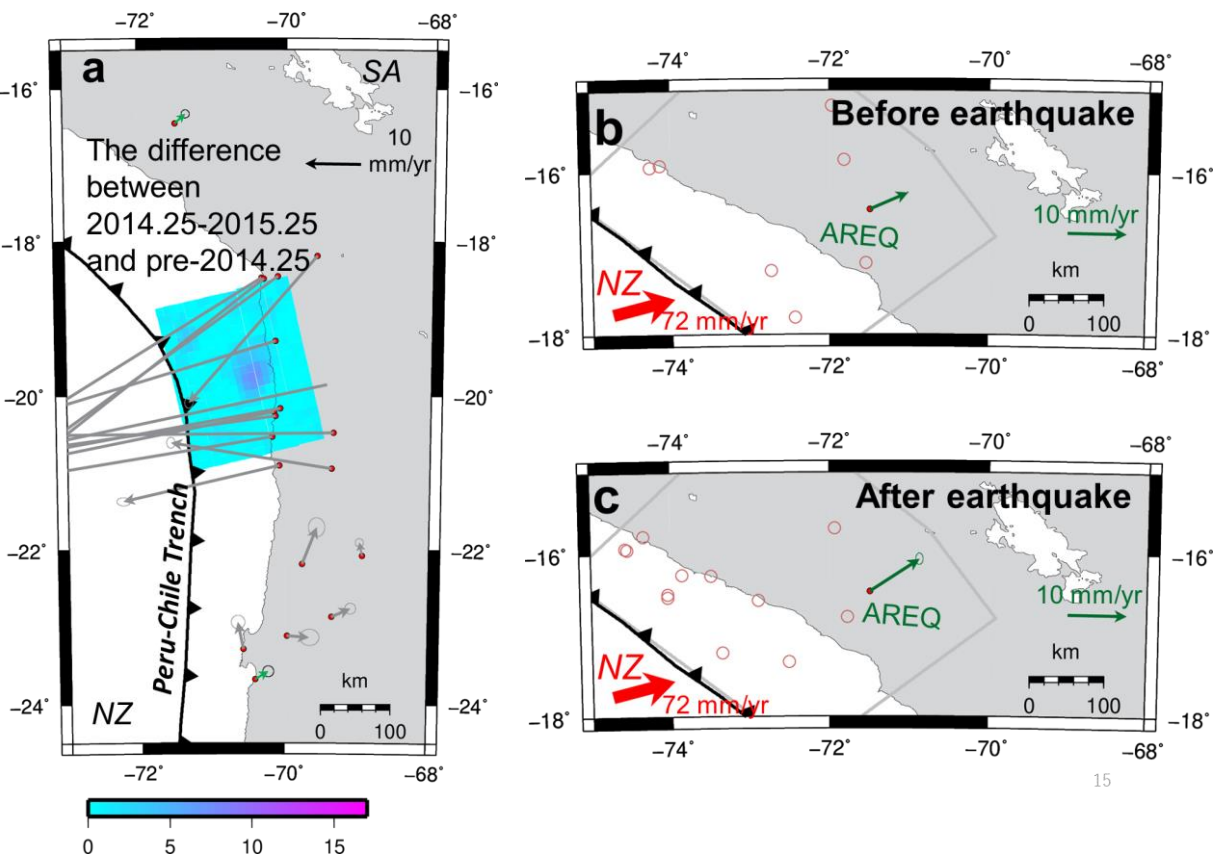


## The 2010 Maule Earthquake (Mw 8.8)

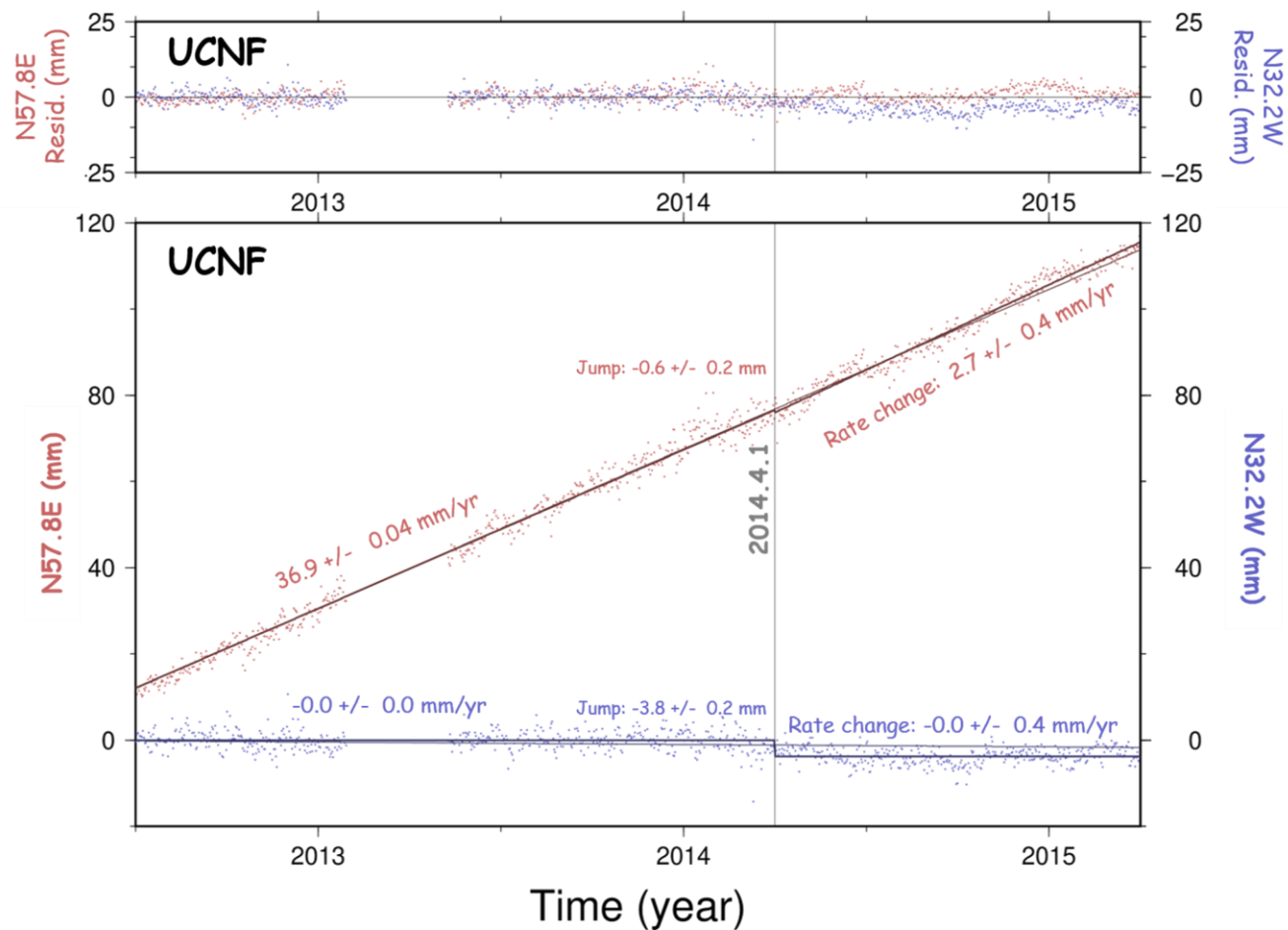


Positive change in the slope of the red time series.





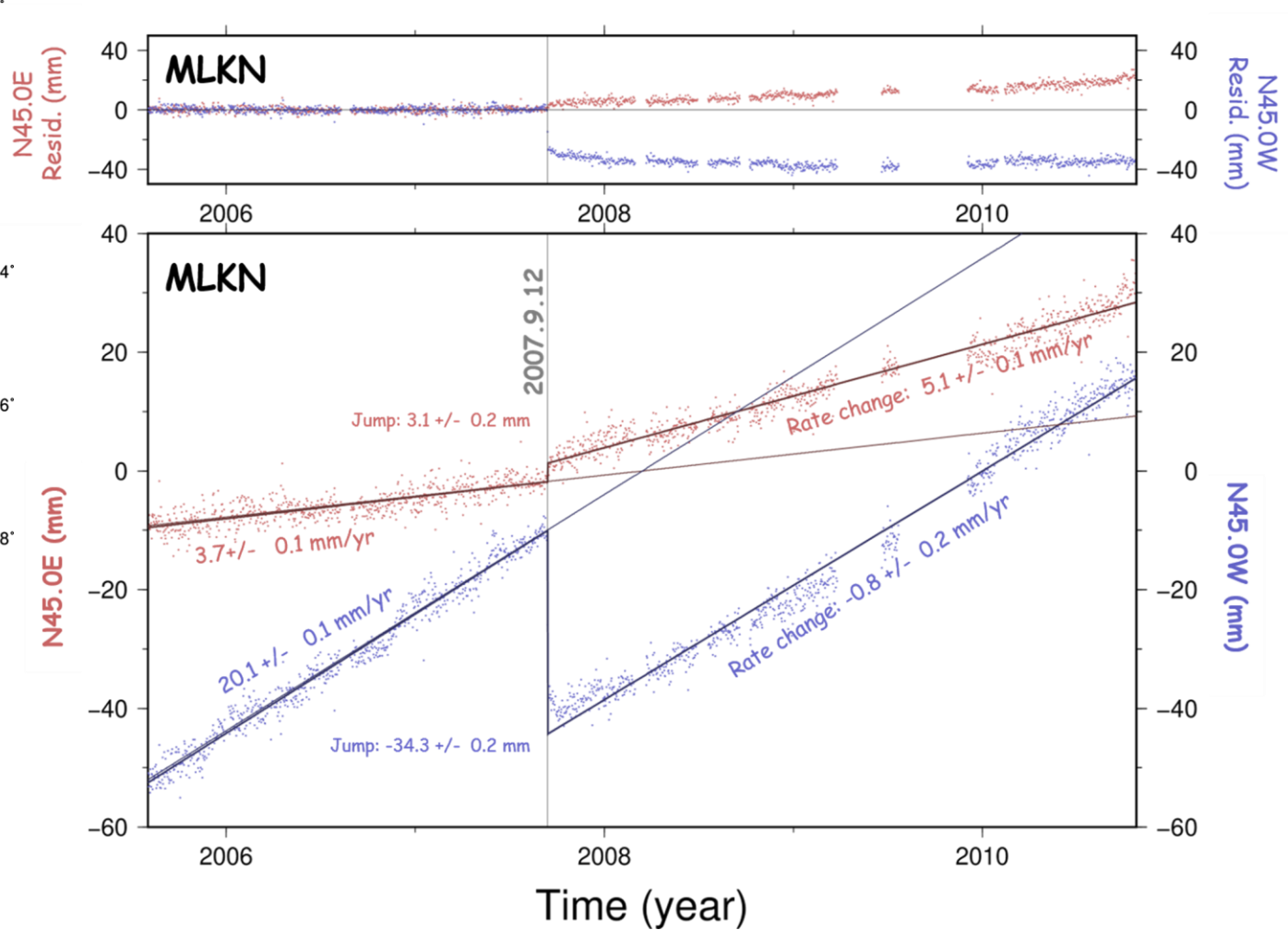
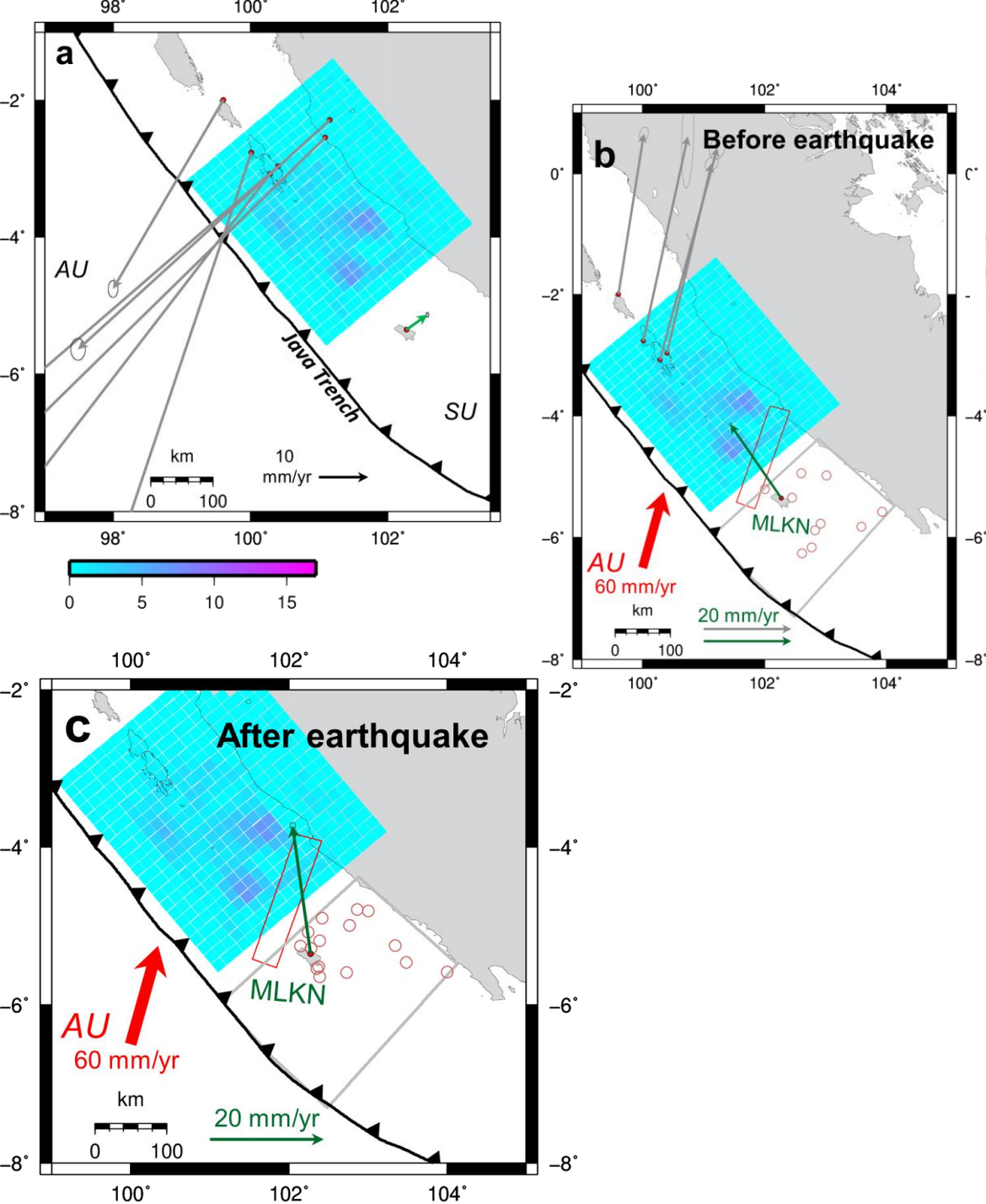
## The 2014 Iquique Earthquake (Mw 8.2)



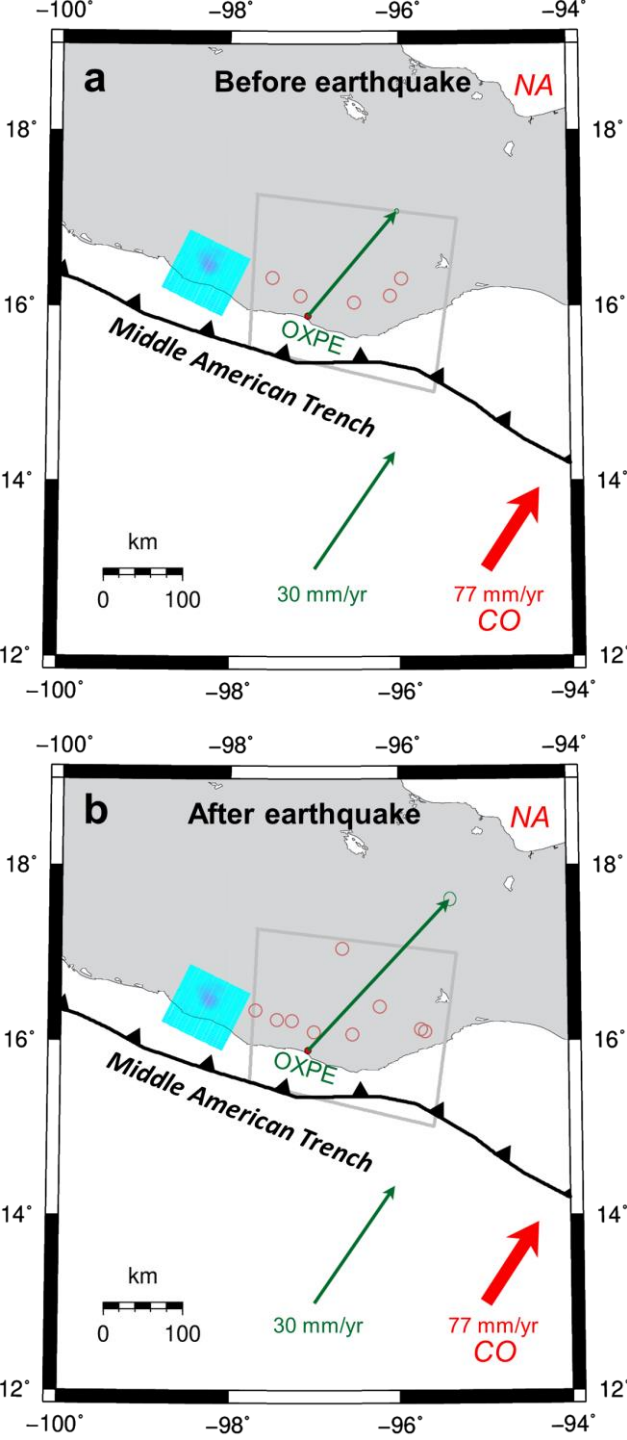
Positive change in the slope of the red time series.



# The 2007 Bengkulu Earthquake (Mw 8.4)

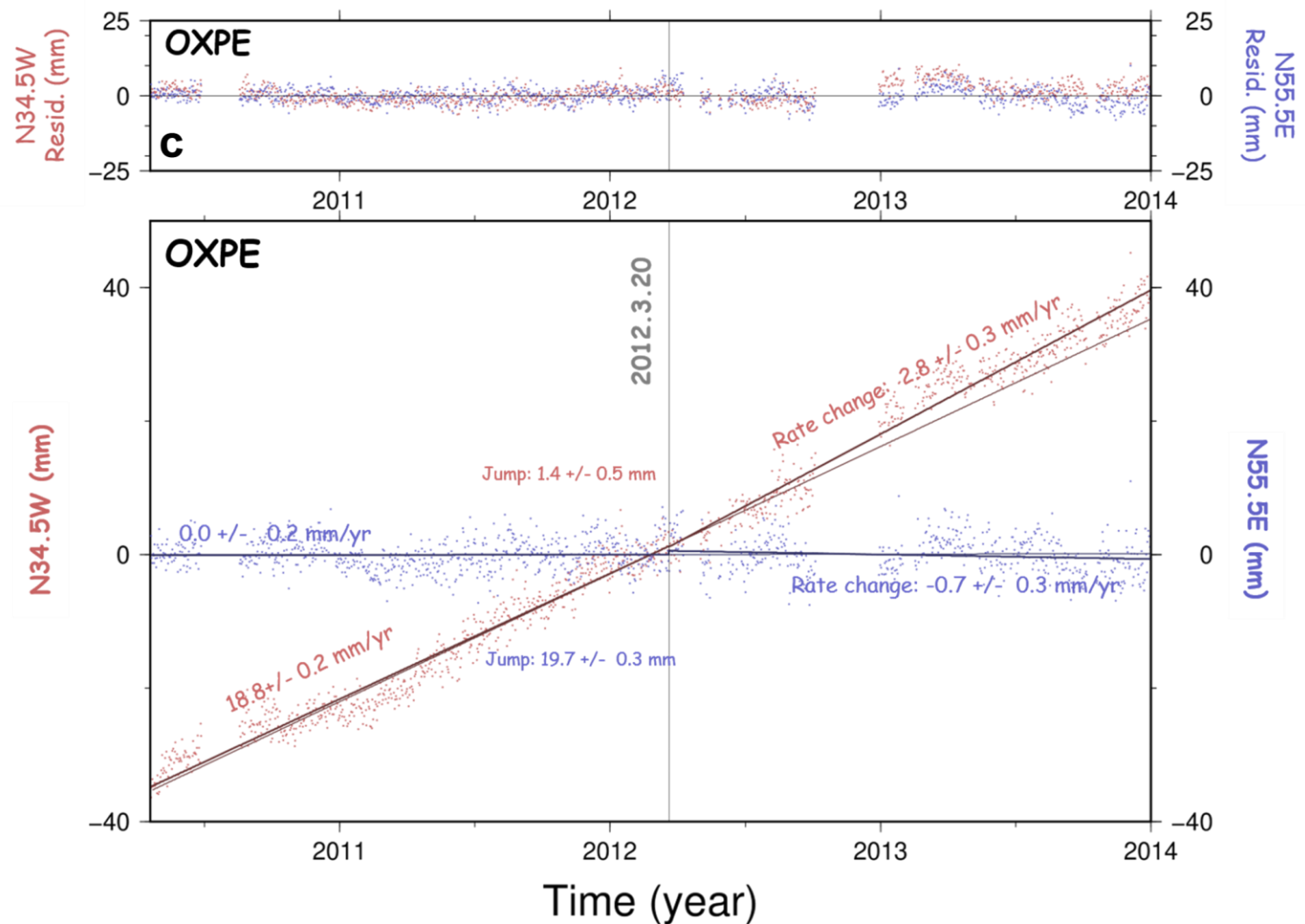


Positive change in the slope of the red time series.



The pre-earthquake landward movement of the GNSS stations has been accelerated after the 2012 Oaxaca earthquake.

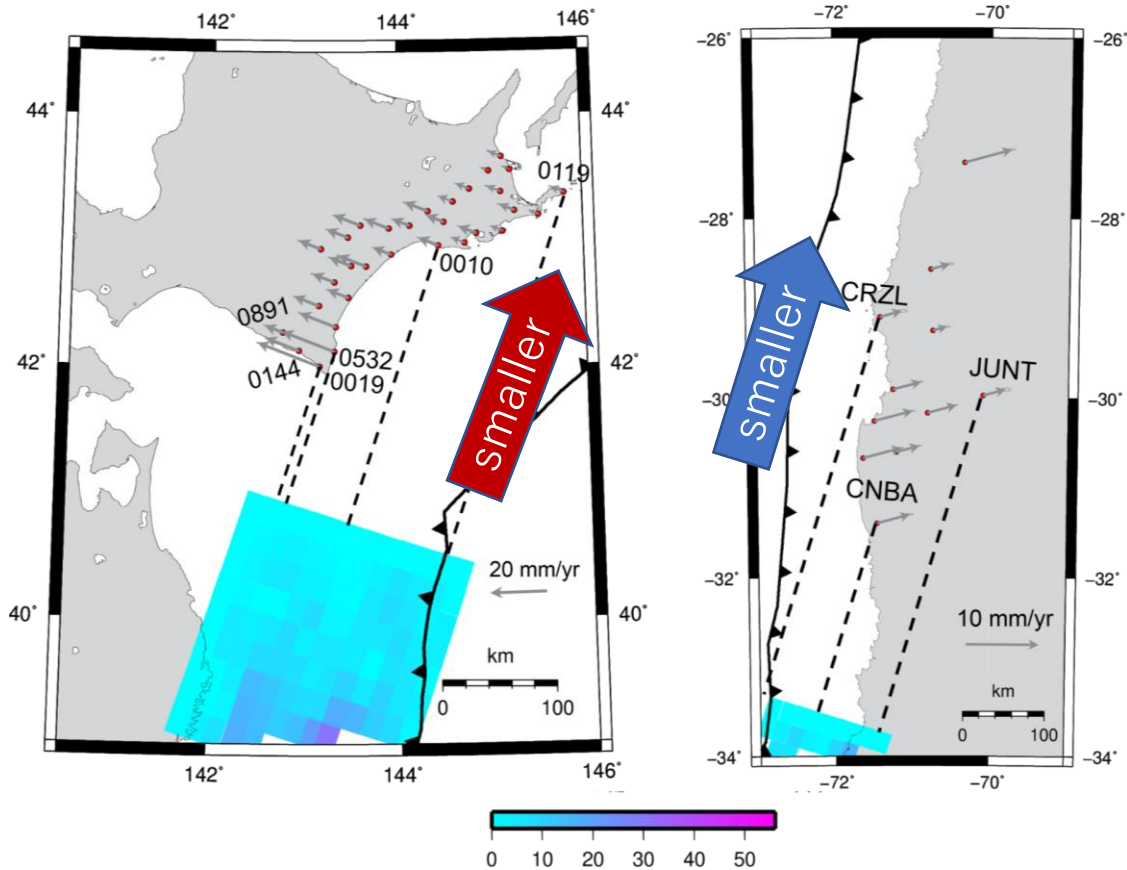
## The 2012 Oaxaca Earthquake (Mw 7.4)



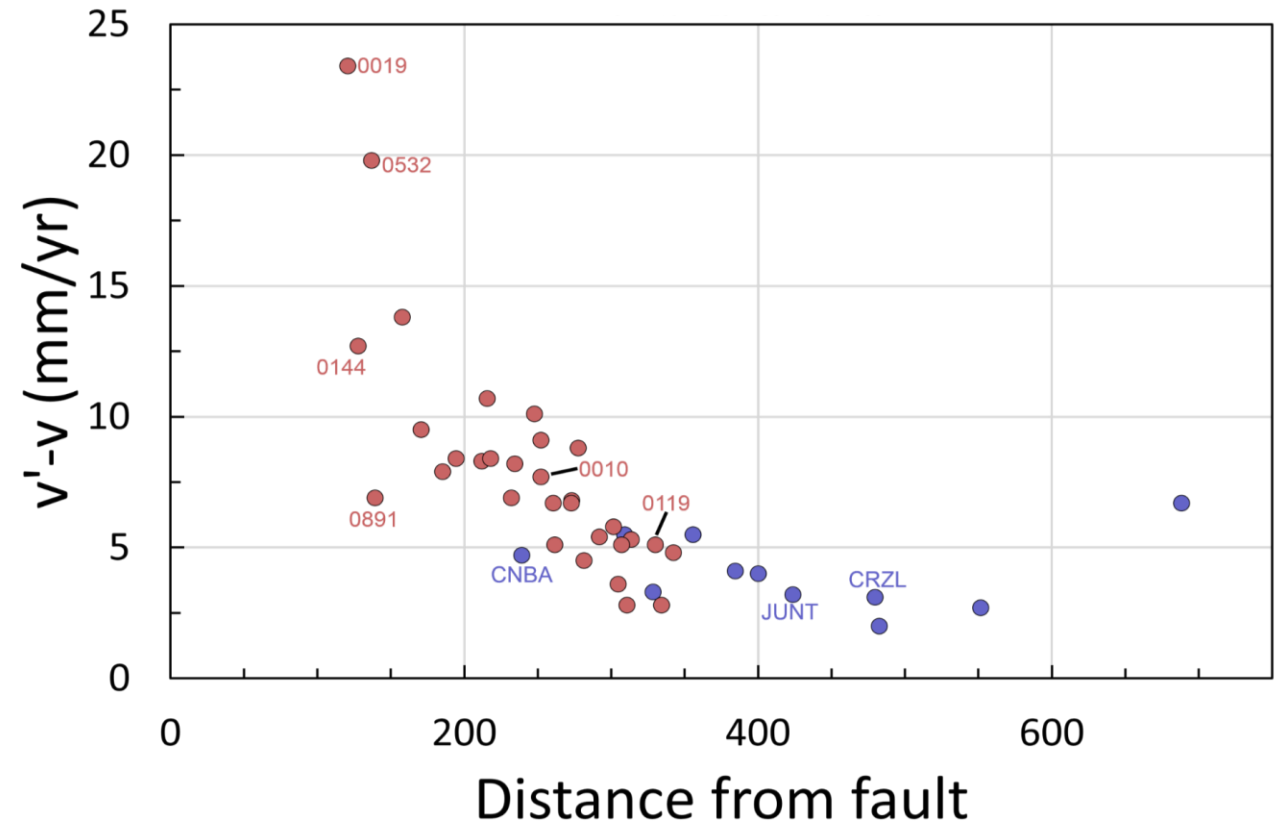
Positive change in the slope of the red time series.

# Summary of observations

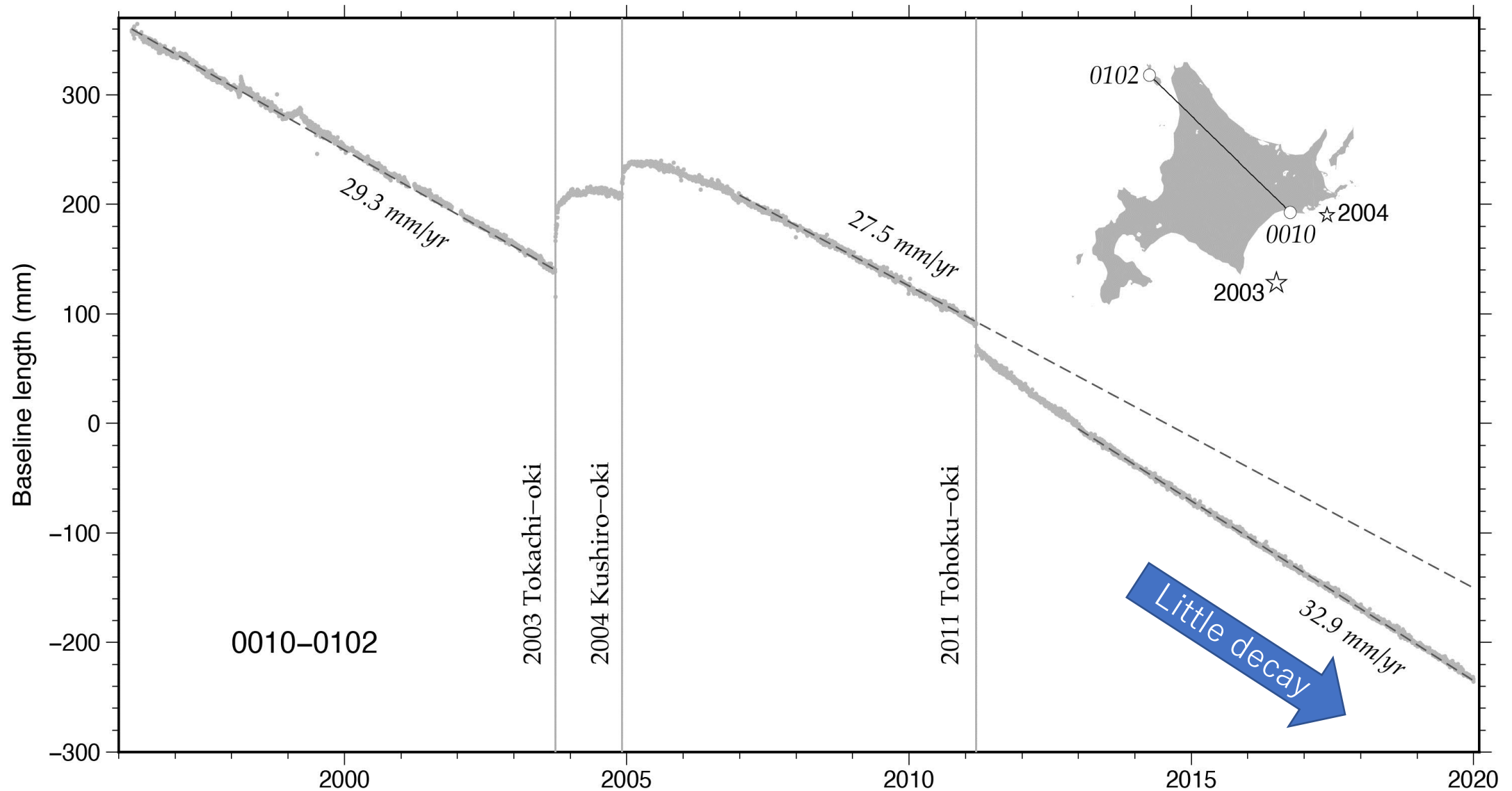
# Spatial decay of the enhanced coupling



These landward velocities decay as we go away from the fault



# Temporal decay of the enhanced coupling



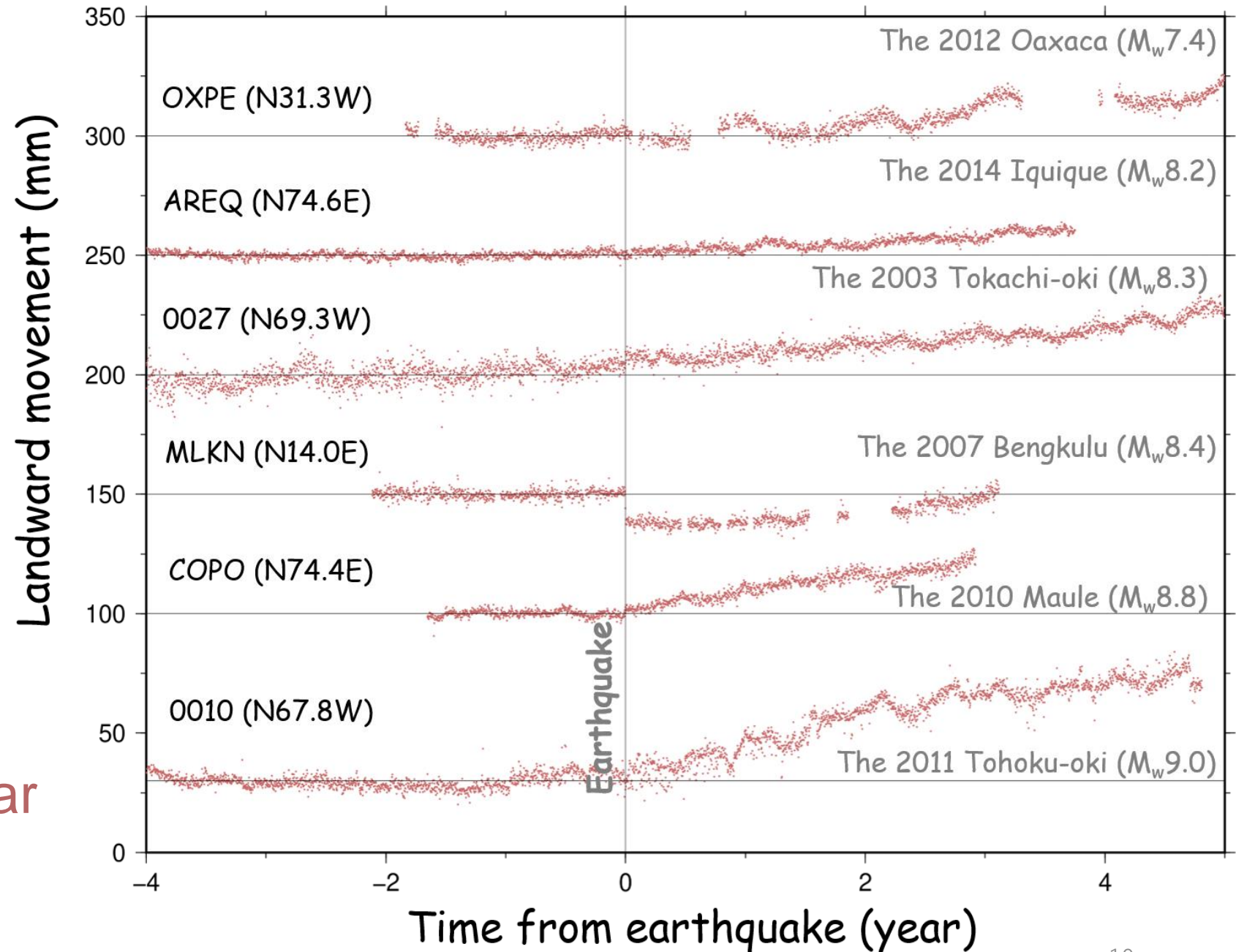
Little temporal decay of the postseismic enhanced coupling after the 2011 Tohoku-oki earthquake.



# Comparison of 6 cases

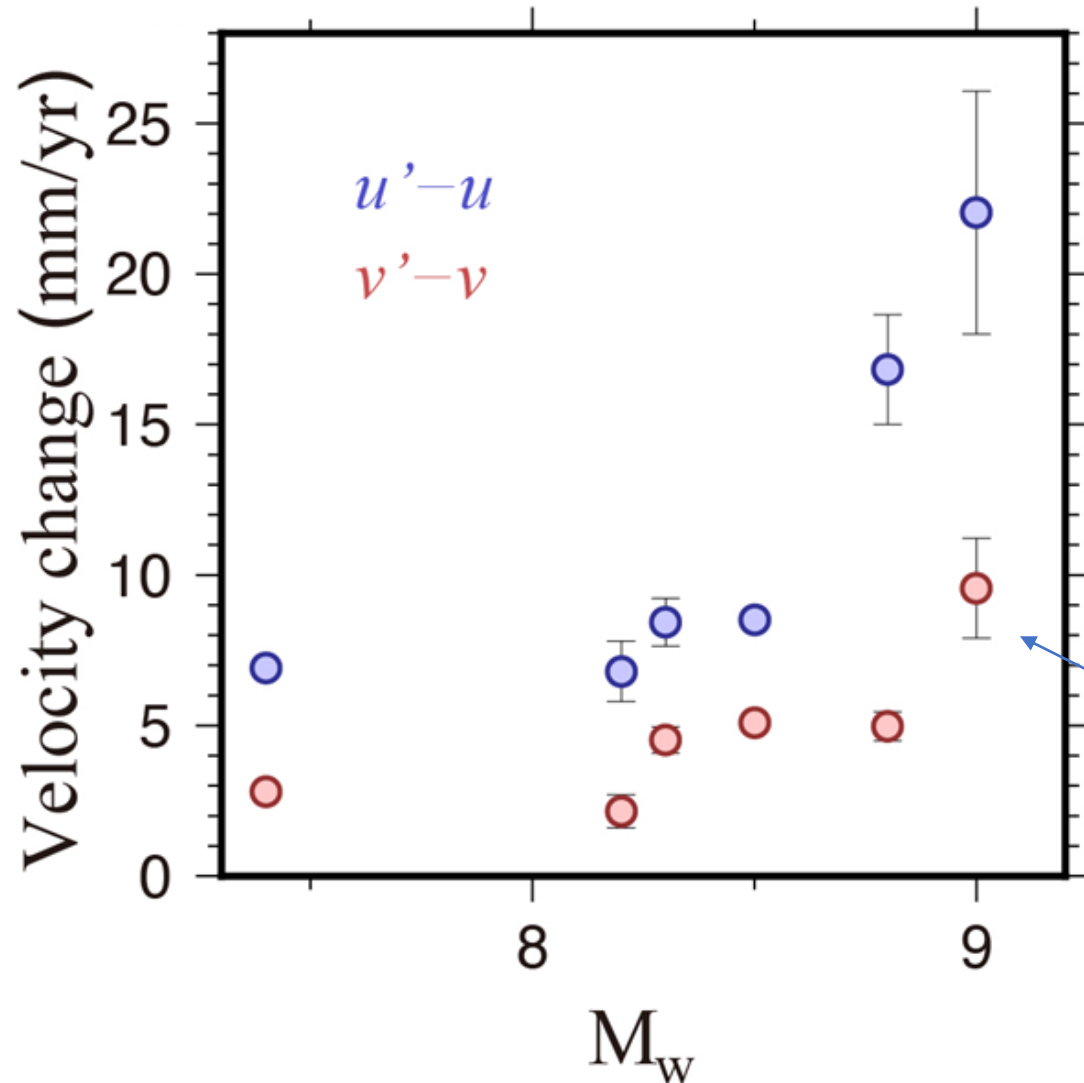
De-trended using parts before earthquakes

$M_w$  dependence is clear



# Discussion: Slab acceleration model

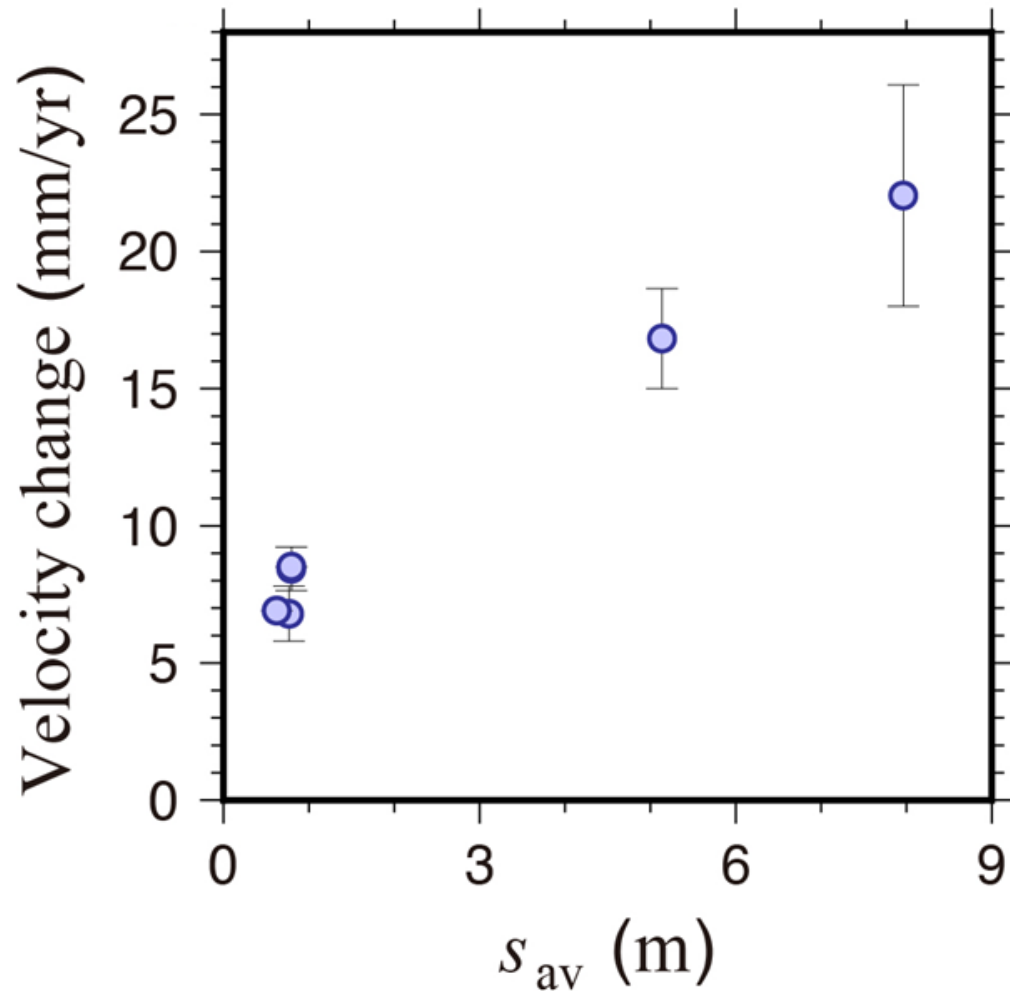
# $M_w$ dependence of acceleration?



We can see that a larger earthquake makes a larger acceleration, both **forearc** ( $v$ ) and **slab** ( $u$ ) velocities.

The average values and 1-sigma standard deviations of  $u' - u$  and  $v' - v$  are given for earthquakes where multiple stations are available.

# Average fault slip $s_{av}$ vs acceleration



Slab acceleration model predicts they are proportional (Heki & Mitsui, 2013)

Good correlation with  $s_{av}$ , but its not clear if they are proportional (4 eqs. with  $M_w \leq 8.5$  are clustered ).

# Conclusions

- Confirmed previous studies for the 2003 Tokachi-oki and the 2011 Tohoku-oki (Heki and Mitsui, 2013) and the 2010 Maule (Melnick et al., 2017) earthquakes.
- Found 6 enhanced coupling cases for 4 subduction zones.
- Studied spatial and temporal decay of the enhancement signature.
- Degree of enhancement positively correlated with  $M_w$ , and possibly scales with average fault slip (Yuzariyadi and Heki, in preparation).



# Acknowledgments

This study was fully supported by Indonesia Endowment Fund for Education (LPDP).

## Appdix 1: Two periods used to estimate velocity changes before and after the earthquakes.

- These periods should be long enough to enable estimation of accurate velocities (>1.0 year) and hopefully be immediately before and after earthquakes.
- Actually, we often have to shift or shorten these periods to avoid unwanted transient movememnts by other smaller earthquakes during the studied periods.

No	Earthquake (M <sub>w</sub> )	Before earthquake	After earthquake <sup>3</sup>
1	2011/3/11 Tohoku-oki (9.0)	2008.00-2011.19	2011.19-2015.00
2	2003/9/25 Tokachi-oki (8.3)	1996.00-2003.74 <sup>1</sup>	2003.74-2010.10
3	2010/2/28 Maule (8.8)	~2008.00 <sup>2</sup> -2010.16	2010.16-2014.70
4	2014/4/1 Iquique (8.2)	~2010.00 <sup>2</sup> -2014.25	2014.25-2015.25
5	2007/9/12 Bengkulu (8.4)	2005.50-2007.70	2007.70-2010.81 <sup>4</sup>
6	2012/3/20 Oaxaca (7.4)	2010.38-2012.22	2012.22-2015.00

<sup>1</sup> Shifted to 1996.0-2003.0 to avoid influence of the Miyagi-oki earthquake (M<sub>w</sub> 7.0) on 2003 May 26 for stations close to its epicenter

<sup>2</sup> Earliest possible starting times used depending on the availability of the stations

<sup>3</sup> The early non-linear postseismic periods avoided to draw Fig for cases of Tohoku-Oki and Tokachi-Oki earthquake case.

<sup>4</sup> Only data until the occurrence of the 2010 Mentawai earthquake.

# Appendix 2: Supporting Data: Seismicity and fault slip distribution

isc.ac.uk/iscbulletin/search/catalogue/

International Seismological Centre

About ISC | ISC Products | ISC Bulletin | ISC-GEM Catalogue

Int. Station Registry | IASPEI GT | Event Bibliography

ISC Bulletin

About

Search the ISC Bulletin

Summary of the Bulletin

Review procedure

ISC locator

Standards & formats

Data collection

Contributing agencies

Collected data

Scanned ISS pages

Citing

ISC Bulletin: event catalogue search

<https://doi.org/10.31905/D808B830>

Now been completely rebuilt for the period 1964-1969 and magnitudes for the entire period of 1964-1969. The location procedure that is currently used is based on the location procedure that is currently used and a considerable number of previously unlocated seismic deployments have been added.

Bulletin search

ISC FDSN Event WS

Event catalogue

Arrivals

Focal mechanisms

Web services

Select database:

☐ Reviewed ISC Bulletin ☒ ISC Bulletin

Output format:

☒ CSV formatted catalogue ☐ QuakeML (XML stream)

USGS

Earthquake Hazards Program

Latest Earthquakes

Overview

Interactive Map

Regional Information

Impact

Felt Report - Tell Us!

Did You Feel It?

ShakeMap

Technical

Origin

Moment Tensor

Focal Mechanism

Finite Fault

Waveforms

Download Event KML

View Nearby Seismicity

Earthquakes

Hazards

Data & Products

Learn

Monitoring

Research

Search...

SEARCH

earthquake.usgs.gov/earthquakes/eventpage/official20110311054624120\_30/finite-fault

M 9.1 - 2011 Great Tohoku Earthquake, Japan

2011-03-11 05:46:24 (UTC) | 38.297°N 142.373°E | 29.0 km depth

Finite Fault

View all finite-fault products (1 total)

Contributed by USGS last updated 2018-10-17 20:34:32 (UTC)

✓ The data below are the most preferred data available

✓ The data below have been reviewed by a scientist

Data Process and Inversion

We used GSN broadband waveforms downloaded from the NEIC waveform server. We analyzed 42 teleseismic broadband P waveforms, 14 broadband SH waveforms, and 61 long period waveforms and are then used to constrain the slip history using a finite fault inverse algorithm (Ji et al., 2002). We begin modeling using a hypocenter matching or adjusted slightly from the time solutions, or the gCMT moment tensor (for historic solutions).

Result

After comparing waveform fits based on the two planes of the input moment tensor, we find that the nodal plane (strike = 198.0°, dip = 15.0°) fits the data better. The seismic moment is 1.1e21 N-m.

Segment	Strike
1	198.0°
2	198.0°
3	198.0°

Cross-section of Slip Distribution

Rupture Front Contours Plotted Every 40 s

Slip (m)

Strike = 198

Distance Along Dip (km)

Distance Along Strike (km)

Depth Relative to Hypocenter (24.4 km)

Cross-section of slip distribution. The strike direction is indicated above each fault

Surface Projection

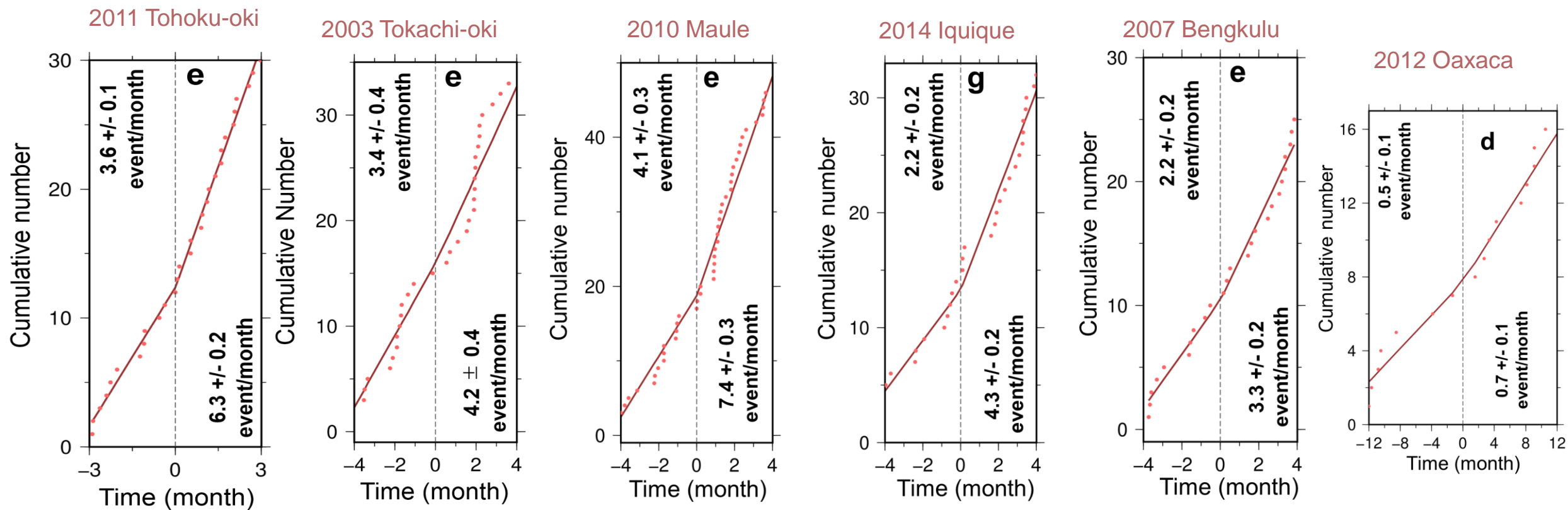
42°

Seismicity with  $M_b \geq 2$  and depth  $\leq 60$  km.

Slip distributions of the megathrust earthquakes.

This slip distribution will be shown in the following figures and will be averaged to get the  $S_{av}$

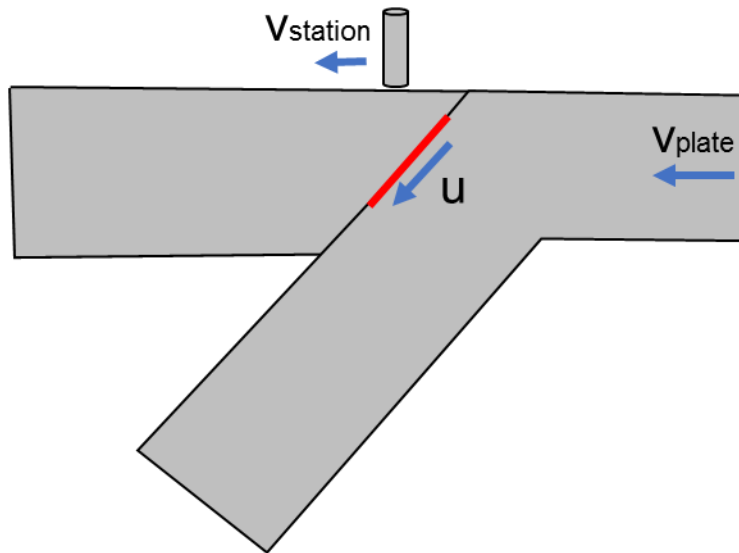
## Appendix 3: Increase in seismicity in the 6 cases



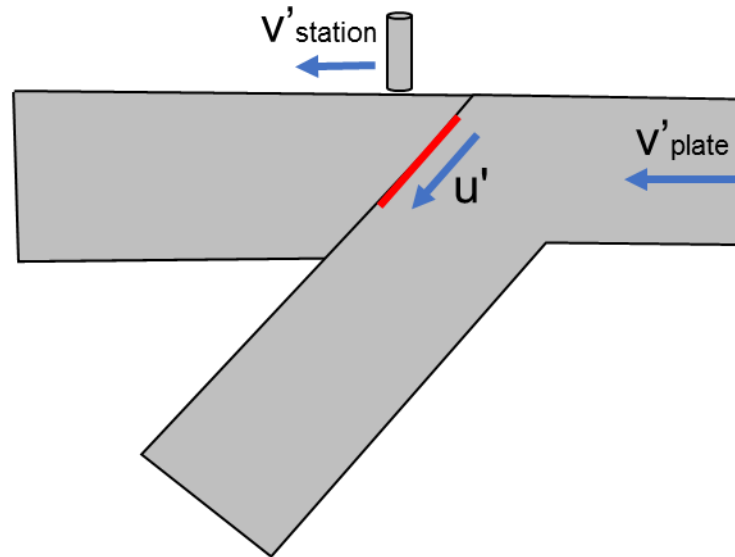
## Appendix 4: Conversion from forearc acceleration $v'-v$ to possible slab acceleration $u'-u$

Generally,  $v$  becomes larger if interplate coupling is stronger, but  $v$  never exceeds  $u$ .

Before earthquake



After earthquake

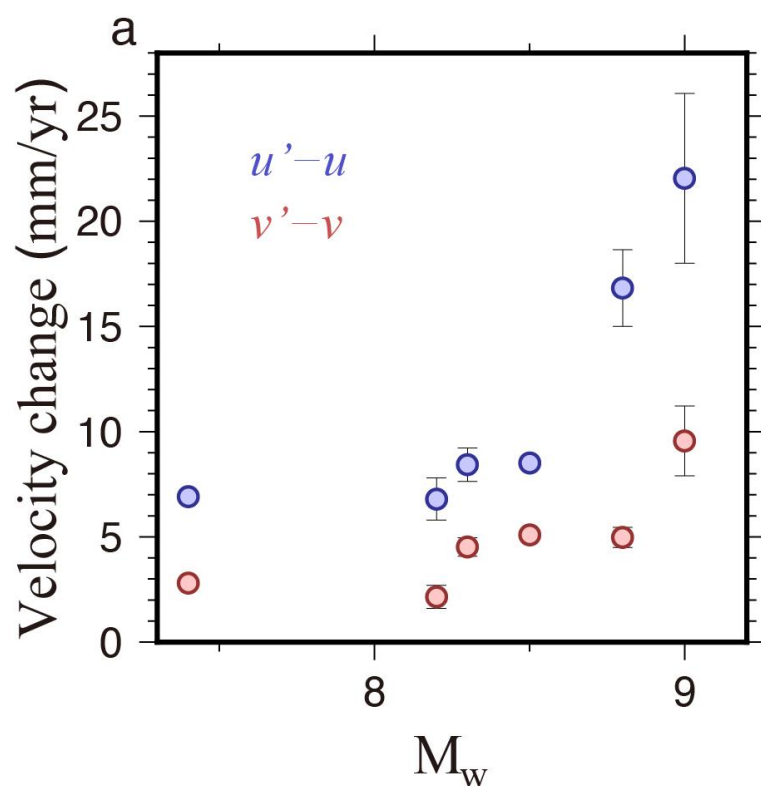


Subduction speed,  $v_{plate}$ , calculated by subtracting the MORVEL model velocities (Argus et al., 2011) from ITRF velocities.

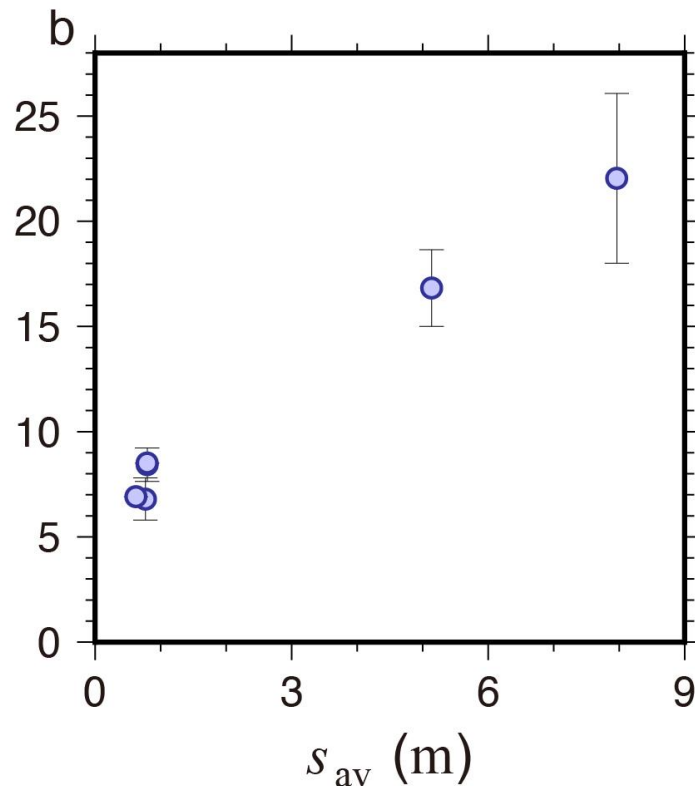
$$u'-u = (v_{plate}/v_{station}) \times (v'_{station} - v_{station})$$



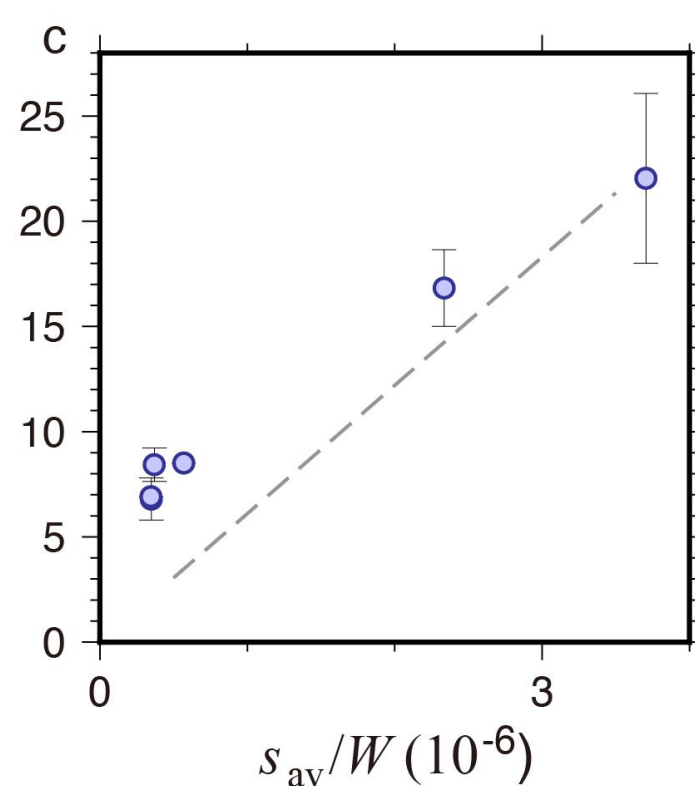
## Appendix 5: Comparison of the data with the slab acceleration model



We can see that a larger earthquake makes a larger acceleration, both **forearc** ( $v$ ) and **slab** ( $u$ ) velocities.



The acceleration seems to show good correlation with  $s_{av}$  but it is not very clear if the two quantities are proportional considering the four earthquakes with  $M_w \leq 8.5$  are clustered and do not contribute to the evaluation of the linearity.



Data in Figure c shows good linearity, but it is not enough to give firm support to the slab acceleration model proposed by Heki and Mitsui (2013), considering that 4 smaller earthquakes make one cluster.